Chapter 2
Equivalent Single Layer Model for Thin Laminated Cylindrical Shells

Abstract In this chapter we consider the equivalent single layer model for thin multi-layered cylindrical shells. It is based on the generalized Timoshenko hypotheses and results in nonlinear governing equations for the whole stacked sequence of an elastic laminated shell. Considering variations of the nonlinear equations, we derive buckling equations of a thin elastic laminated shell loaded with static conservative loads. The derived dynamic equations are adapted for the case when a shell is assembled from elastic and viscoelastic layers with properties represented by a complex shear modulus. Viscoelastic layers or cores are assumed to be made of smart materials, such as magnetorheological elastomers and electrorheological composites. The reader can become acquainted with elastic and rheological properties of some smart viscoelastic materials which may be used as damping elements of smart thin-walled laminated shells.

2.1 Equations of Thin Elastic Laminated Cylindrical Shells

In this section we consider principle hypotheses for the two-dimensional theory taking into account transverse shear, the strain-displacement and constitutive relations. Applying a mixed variational principle, the nonlinear equations describing the motion of an elastic laminated cylindrical shell and the natural boundary conditions as well are deduced. For cases when vibrations occur with formation of short waves, the full system of equations is reduced to the simplified system of three differential equations for the stress, displacement and shear functions. The edge effect equations taking into account transverse shear are obtained. The asymptotic error of the derived equations is shortly discussed.

G. I. Mikhasev and H. Altenbach, *Thin-walled Laminated Structures*,
Advanced Structured Materials 106, https://doi.org/10.1007/978-3-030-12761-9_2

2.1.1 Laminated Cylindrical Shell

Consider a thin non-circular laminated cylindrical shell (s. Fig. 2.1) consisting of N transversely isotropic layers characterized by the following parameters: length L, thickness h_k, density ρ_k, Young's modulus E_k, shear modulus G_k, and Poisson's ratio ν_k, where $k = 1, 2, \ldots, N$ are the number of layers. It is assumed that each layer has a constant thickness.

The middle surface of any fixed layer is taken as the reference surface. We introduce a local orthogonal coordinate system by means of unit vectors $\boldsymbol{e}_1, \boldsymbol{e}_2$ and $\boldsymbol{n} = \boldsymbol{e}_1 \times \boldsymbol{e}_2$ with origin in the point O as shown in Fig. 2.1. Let α_1 and α_2 be the axial and circumferential coordinates, respectively, and $\alpha_3 = z$ is the normal coordinate. The radius of curvature of the reference surface is $R_2 = 1/k_{22}(\alpha_2)$. The shell is bounded by two not necessarily plane edges

$$\alpha_1^*(\alpha_2) \leq \alpha_1 \leq \alpha_1^{**}(\alpha_2) \tag{2.1}$$

and may be not closed in the direction of α_2 (the case of a non-circular cylindrical panel).

In this section, we assume that every layer is made of an elastic material which may be inhomogeneous. Then the Young's moduli E_k and Poisson's ratios ν_k are real numbers which may depend on the curvilinear coordinates α_1, α_2. Below, laminated shells and sandwiches with viscoelastic layers and cores will be also considered. In particular, we discuss the case when a sandwich is formed by embedding a magnetorheological elastomer or electrorheological composite between elastic layers. In this case parameters E_k and G_k corresponding to the viscoelastic laminas with adaptive elastic and viscous properties will be considered as complex functions of α_1, α_2 and time t.

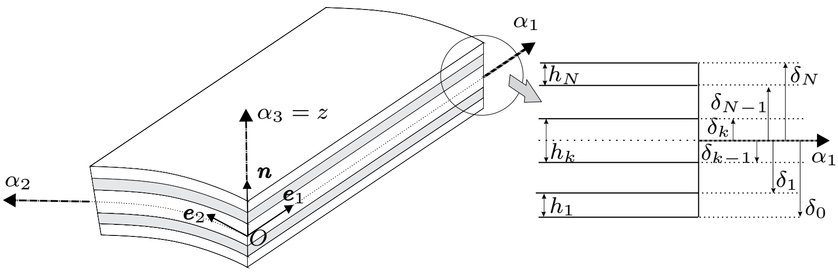

Fig. 2.1 Laminated cylindrical shell with a curvilinear coordinate system.

2.1.2 Principal Hypotheses

Now we introduce some additional notations. Let $z = \delta_k$ be the coordinate of the upper bound of the k^{th} layer, and $z = \delta_0$ is the coordinate of the inner surface of the shell, u_i and w are the tangential and normal displacements of points on the reference surface of the shell, respectively,

$$h = \sum_{k=1}^{N} h_k$$

is the total thickness of the laminate, $u_i^{(k)}$ are the tangential displacements of points of the k^{th} layer, σ_{i3} are the transverse shear stresses (s. Fig. 2.2), θ_i are the angles of rotation of the normal $\boldsymbol{n}$ about the vector $\boldsymbol{e}_i$ (s. Fig. 2.1). Here $i = 1, 2$; $k = 1, 2, \ldots, N$.

The following hypotheses of the laminated shell theory stated in Grigolyuk and Kulikov (1988) are assumed here:

1. The distribution law of the transverse tangent stresses across the thickness of the k^{th} layer is assumed to be of the form

$$\sigma_{i3} = f_0(z)\mu_i^{(0)}(\alpha_1, \alpha_2, t) + f_k(z)\mu_i^{(k)}(\alpha_1, \alpha_2, t) , \tag{2.2}$$

where t is time, $f_0(z), f_k(z)$ are continuous functions introduced as follows

$$\begin{aligned} f_0(z) &= \frac{1}{h^2}(z - \delta_0)(\delta_N - z) \quad \text{for } z \in [\delta_0, \delta_N], \\ f_k(z) &= \frac{1}{h_k^2}(z - \delta_{k-1})(\delta_k - z) \text{ for } z \in [\delta_{k-1}, \delta_k], \\ f_k(z) &= 0 \qquad\qquad\qquad\qquad \text{for } z \notin [\delta_{k-1}, \delta_k]. \end{aligned} \tag{2.3}$$

2. Normal stresses acting on the area elements parallel to the original one are negligible with respect to the other components of the stress tensor.

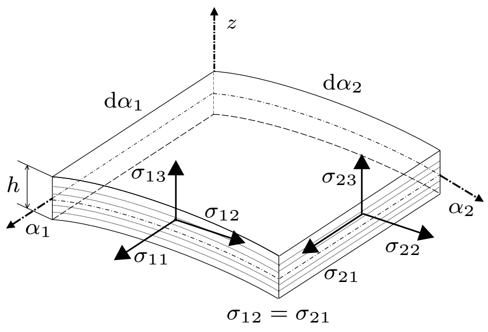

Fig. 2.2 Infinitesimal element of a laminated shell, reference surface and stresses (after Mikhasev and Botogova, 2017).

3. The deflection $w(\alpha_1, \alpha_2, t)$ does not depend on the coordinate z.
4. The tangential (in-plane) displacements are distributed across thickness of the layer package according to the generalized kinematic Timoshenko hypotheses

$$u_i^{(k)}(\alpha_1, \alpha_2, z, t) = u_i(\alpha_1, \alpha_2, t) + z\theta_i(\alpha_1, \alpha_2, t) + g(z)\psi_i(\alpha_1, \alpha_2, t), \quad (2.4)$$

where

$$g(z) = \int\limits_0^z f_0(x)\mathrm{d}x.$$

In Eq. (2.4), ψ_i are required parameters characterizing the transverse shear in the shell. Hypothesis (2.4) permits to describe the non-linear dependence of the tangential displacements on z; at $g \equiv 0$ it turns into the linear Timoshenko hypotheses coinciding with the classical Kirchhoff-Love hypotheses if θ_i are functions of the tangential displacements and derivatives of the deflection.

In what follows, it will be shown that the functions $\mu_i^{(0)}(\alpha_1, \alpha_2), \mu_i^{(k)}(\alpha_1, \alpha_2)$ are coupled with the vector $\bar{\Psi} = (\psi_1, \psi_2)^{\mathrm{T}}$ and depend on elements of a matrix characterizing the shear deformability of the k^{th} layer. So, in the theory developed by Grigolyuk and Kulikov (1988) and based on the above hypothesis, the five components $w, u_i, \psi_i (i = 1, 2)$ are assumed to be independent functions, and θ_i are defined in the derivatives of the deflection w.

2.1.3 Strain-displacement Relations

We assume that the shell deformation under buckling or vibrations is accompanied by the formation of a large number of waves so that the shell may be considered as shallow one within the limits of one half-wave. Then, $\theta_i \approx -w_{,i}$, and taking into account the hypotheses accepted above, the strain-displacement relations will be as follows (Grigolyuk and Kulikov, 1988):

$$u_i^{(k)} = u_i - zw_{,i} + g(z)\psi_i, \qquad i, j = 2, \quad (2.5)$$

$$\epsilon_{ij} = e_{ij} + z\,\kappa_{ij} + g(z)\psi_{ij}, \;\; \epsilon_{i3} = f_0(z)\psi_i, \quad (2.6)$$

where

$$\begin{aligned} e_{ij} &= \frac{1}{2}(u_{i,j} + u_{j,i} + w_{,i}w_{,j}) + k_{ij}w, \\ \psi_{ij} &= \frac{1}{2}(\psi_{i,j} + \psi_{j,i}), \quad \kappa_{ij} = -w_{,ij}, \\ k_{11} &= k_{12} = 0, \quad k_{22} = \frac{1}{R_2(\alpha_2)}. \end{aligned} \quad (2.7)$$

Here, the differentiation with respect to the coordinate α_i is designated as $(\ldots)_{,i}$.

2.1.4 Constitutive Equations for Elastic Materials

Let us introduce the vectors

$$\bar{\sigma} = (\sigma_{11}, \sigma_{22}, \sigma_{12})^{\mathrm{T}}, \quad \bar{\epsilon} = (\epsilon_{11}, \epsilon_{22}, \epsilon_{12})^{\mathrm{T}} \tag{2.8}$$

of the tangential (with respect to the original surface) stresses and strains in the k^{th} elastic layer for the plane stress state. When taking the static hypothesis (2.2) into account, these stresses and strains are linked by Hooke's law

$$\bar{\epsilon} = \mathbf{A}^{(k)}\bar{\sigma}, \tag{2.9}$$

where

$$\mathbf{A}^{(k)} = \begin{pmatrix} a_{11}^{(k)} & a_{12}^{(k)} & a_{16}^{(k)} \\ a_{12}^{(k)} & a_{22}^{(k)} & a_{26}^{(k)} \\ a_{16}^{(k)} & a_{26}^{(k)} & a_{66}^{(k)} \end{pmatrix} \tag{2.10}$$

is the 3×3 matrix of the plane compliances for the k^{th} layer. If the layer is isotropic , then

$$a_{11}^{(k)} = a_{22}^{(k)} = \frac{1}{E_k}, \quad a_{12}^{(k)} = -\frac{\nu_k}{E_k}, \quad a_{66}^{(k)} = \frac{1+\nu_k}{E_k}, \quad a_{16}^{(k)} = a_{26}^{(k)} = 0 \tag{2.11}$$

and the constitutive equation (2.9) for the generalized plane stress state may be rewritten as it follows

$$\sigma_{ij} = \frac{E_k}{1-\nu_k^2}\Xi\epsilon_{ij}, \quad i,j = 1,2, \tag{2.12}$$

where

$$\Xi\epsilon_{ij} = (1-\nu)\epsilon_{ij} + \nu\delta_{ij}(\epsilon_{11}+\epsilon_{22}), \tag{2.13}$$

δ_{ij} is the Kronecker symbol ($\delta_{ii} = 1$; $\delta_{ij} = 0, i \neq j$), and

$$\nu = \sum_{k=1}^{N} \frac{E_k h_k \nu_k}{1-\nu_k^2} \left(\sum_{k=1}^{N} \frac{E_k h_k}{1-\nu_k^2} \right)^{-1} \tag{2.14}$$

is the reduced Poisson's ratio for the whole stacked sequence (Grigolyuk and Kulikov, 1988).

The transverse shear stresses σ_{i3} have to satisfy the following matrix equation

$$\bar{\epsilon}_3 = \mathbf{A}_3^{(k)}\bar{\sigma}_3, \tag{2.15}$$

where

$$\bar{\sigma}_3 = (\sigma_{13}, \sigma_{23})^{\mathrm{T}}, \quad \bar{\epsilon}_3 = (\epsilon_{13}, \epsilon_{23})^{\mathrm{T}} \tag{2.16}$$

and

$$\mathbf{A}_3^{(k)} = \begin{pmatrix} a_{55}^{(k)} & a_{45}^{(k)} \\ a_{45}^{(k)} & a_{44}^{(k)} \end{pmatrix} \tag{2.17}$$

is the 2×2 matrix of the transverse shear compliances. For a isotropic layer, $a_{45}^{(k)} = 0, a_{55}^{(k)} = a_{44}^{(k)} = G_k^{-1}$. It is obvious that because of the accepted hypotheses (2.2), the constitutive equation (2.15) is not satisfied. However, it will be shown below that Eq. (2.15) may be satisfied integrally with some weight function for the thickness of the laminated package.

We also introduce the reduced Young's modulus

$$E = \frac{1-\nu^2}{h} \sum_{k=1}^{N} \frac{E_k h_k}{1-\nu_k^2}, \tag{2.18}$$

and the dimensionless stiffness characteristics

$$\gamma_k = \frac{E_k h_k}{1-\nu_k^2} \left(\sum_{k=1}^{N} \frac{E_k h_k}{1-\nu_k^2} \right)^{-1} \tag{2.19}$$

of the k^{th} layer. Then, from Eqs. (2.18) and (2.19) one obtains

$$\frac{E_k h_k}{1-\nu_k^2} = \frac{Eh}{1-\nu^2} \gamma_k \tag{2.20}$$

for any $k = 1, \ldots, N$. The parameters γ_k are important in the estimation of the error of governing equations derived below. In what follows, we assume that the stiffness characteristics γ_k for all layers are approximately the same. In the common case, when a material of some layer is inhomogeneous, the reduced modulus E and Poisson's ratio ν are functions of the curvilinear coordinates.

2.1.5 Stress Resultants

Let T_{ij}, Q_i and M_{ij} be the classical stress resultants (s. Fig. 2.3) which are introduced in the standard way as

$$T_{ij} = \sum_{k=1}^{N} \int_{\delta_{k-1}}^{\delta_k} \sigma_{ij} \, \mathrm{d}z, \quad Q_i = \sum_{k=1}^{N} \int_{\delta_{k-1}}^{\delta_k} \sigma_{i3} \, \mathrm{d}z, \quad M_{ij} = \sum_{k=1}^{N} \int_{\delta_{k-1}}^{\delta_k} z \, \sigma_{ij} \, \mathrm{d}z. \tag{2.21}$$

In addition to the classical resultants, we introduce the generalized stress resultants (Grigolyuk and Kulikov, 1988):

- the generalized transverse shear forces

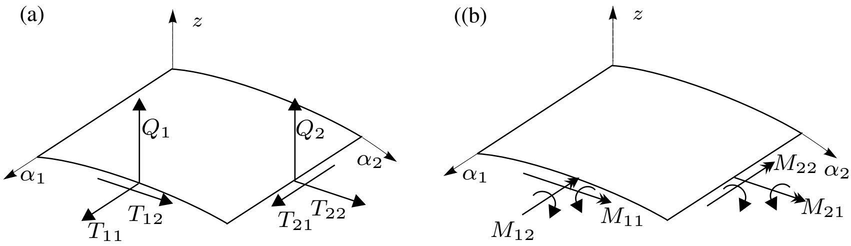

Fig. 2.3 Reference surface. Stress resultants: (a) in-plane forces T_{ij} and transverse shear forces Q_i, (b) moments M_{ij}.

$$Q_{0i} = \sum_{k=1}^{N} \int_{\delta_{k-1}}^{\delta_k} f_0(z)\sigma_{i3}\,\mathrm{d}z, \tag{2.22}$$

- and the generalized moments

$$L_{ij} = \sum_{k=1}^{N} \int_{\delta_{k-1}}^{\delta_k} g(z)\sigma_{ij}\,dz. \tag{2.23}$$

The introduction of the generalized forces and moments is caused by the presence of additional degrees of freedom corresponding to the transverse shear in the shell.

Taking into account Eqs. (2.12)-(2.14), (2.18), Eqs. (2.21), (2.23) can be rewritten

$$\begin{aligned} T_{ij} &= \frac{Eh}{1-\nu^2}\Xi e_{ij} + \frac{Eh^2}{2(1-\nu^2)}\left(c_{13}\Xi\kappa_{ij} + c_{12}\Xi\psi_{ij}\right), \\ M_{ij} &= \frac{1}{2}hc_{13}T_{ij} + \frac{Eh^2}{2(1-\nu^2)}\left(\eta_3\Xi\kappa_{ij} + \eta_2\Xi\psi_{ij}\right), \\ L_{ij} &= \frac{1}{2}hc_{12}T_{ij} + \frac{Eh^2}{2(1-\nu^2)}\left(\eta_2\Xi\kappa_{ij} + \eta_1\Xi\psi_{ij}\right), \end{aligned} \tag{2.24}$$

where

$$\begin{aligned} &c_{12} = \sum_{k=1}^{N} \xi_k^{-1}\pi_{3k}\gamma_k, \quad c_{13} = \sum_{k=1}^{N}(\zeta_{k-1}+\zeta_k)\gamma_k, \\ &\frac{1}{12}h^3\pi_{1k} = \int_{\delta_{k-1}}^{\delta_k} g^2(z)\mathrm{d}z,\ \frac{1}{12}h^3\pi_{2k} = \int_{\delta_{k-1}}^{\delta_k} z\,g(z)\mathrm{d}z,\ \frac{1}{2}h^2\pi_{3k} = \int_{\delta_{k-1}}^{\delta_k} g(z)\mathrm{d}z, \\ &\eta_1 = \sum_{k=1}^{N} \xi_k^{-1}\pi_{1k}\gamma_k - 3c_{12}^2,\ \eta_2 = \sum_{k=1}^{N} \xi_k^{-1}\pi_{2k}\gamma_k - 3c_{12}c_{13}, \\ &\eta_3 = 4\sum_{k=1}^{N}\left(\xi_k^2 + 3\zeta_{k-1}\zeta_k\right)\gamma_k - 3c_{13}^2,\ h\xi_k = h_k,\ h\zeta_n = \delta_n\ (n=0,\,k) \end{aligned} \tag{2.25}$$

Equations (2.24) differ from similar equations for homogeneous shells. They contain terms depending on torsion of the original surface and shear as well. The presence of these terms is not desirable. To eliminate them, we follow Grigolyuk and Kulikov (1988) and introduce the so-called generalized displacements and strains

$$\begin{aligned} u_i &= \hat{u}_i + \frac{1}{2} h c_{13} w_{,\,i} - \frac{1}{2} h c_{12} \psi_i, \\ e_{ij} &= \hat{e}_{ij} - \frac{1}{2} h c_{13} \kappa_{ij} - \frac{1}{2} h c_{12} \psi_{ij}. \end{aligned} \tag{2.26}$$

Then Eq. (2.24) for T_{ij} may be rewritten in terms of the generalized strains as follows

$$T_{ij} = \frac{Eh}{1-\nu^2} \Xi \hat{e}_{ij}. \tag{2.27}$$

Let us consider the following transformations (Grigolyuk and Kulikov, 1988)

$$\hat{M}_{ij} = M_{ij} - \frac{1}{2} h c_{13} T_{ij}, \quad \hat{L}_{ij} = L_{ij} - \frac{1}{2} h c_{12} T_{ij}. \tag{2.28}$$

They lead to equations for the so-called reduced moments and generalized moments

$$\begin{aligned} \hat{M}_{ij} &= \frac{Eh^3}{12(1-\nu^2)} \left(\eta_3 \Xi \kappa_{ij} + \eta_2 \Xi \psi_{ij} \right), \\ \hat{L}_{ij} &= \frac{Eh^3}{12(1-\nu^2)} \left(\eta_2 \Xi \kappa_{ij} + \eta_1 \Xi \psi_{ij} \right). \end{aligned} \tag{2.29}$$

The substitution of (2.2), (2.3) into (2.22) results in the following equations for the generalized shear stress resultants

$$Q_{0i} = \sum_{k=1}^{N} \left(\lambda_k \mu_i^{(0)} + \lambda_{k0} \mu_i^{(k)} \right), \quad i = 1, 2; \tag{2.30}$$

$$\lambda_k = \int\limits_{\delta_{k-1}}^{\delta_k} f_0^2(z) \mathrm{d}z, \qquad \lambda_{kn} = \int\limits_{\delta_{k-1}}^{\delta_k} f_k(z) f_n(z) \mathrm{d}z \qquad (n = 0, k).$$

It will be shown later that they may be expressed in terms of the functions ψ_i.

2.1.6 Mixed Variational Principle

To derive the equations of equilibrium we shall apply to the following mixed variational principle

$$\delta \Pi = \delta A_1^* + \delta A_2^*, \tag{2.31}$$

where A_1^* and A_2^* are the work of both external surface and boundary forces, respectively, and the functional $\varPi$ is defined as (Grigolyuk and Kulikov, 1988)

$$\varPi = \iint\limits_{\mathcal{D}} \left[\sum_{k=1}^{N} \int\limits_{\delta_{k-1}}^{\delta_k} \left(\bar{\sigma}^{\mathrm{T}} \bar{\epsilon} + \bar{\sigma}_3^{\mathrm{T}} \bar{\epsilon}_3 - W_k \right) (1 + k_{22} z)\, \mathrm{d}z \right] \mathrm{d}\alpha_1 \mathrm{d}\alpha_2 . \tag{2.32}$$

In (2.32),

$$W_k = \frac{1}{2} \left(\bar{\sigma}^{\mathrm{T}} \mathbf{A}^{(k)} \bar{\sigma} + \bar{\sigma}_3^{\mathrm{T}} \mathbf{A}_3^{(k)} \bar{\sigma}_3 \right) \tag{2.33}$$

is the strain-energy function of the k^{th} layer, and $\mathcal{D}$ is the domain of the reference surface bounded by a closed curve (s. Fig. 2.4)

$$\varGamma_{\mathcal{D}} = \varGamma_1 \cup \varGamma_2 ,$$

where

$$\begin{array}{l} \varGamma_1 = \varGamma_1^* \cup \varGamma_1^{**}, \quad \varGamma_1^* = \{(\alpha_1, \alpha_2) : \alpha_1 = \alpha_1^*(\alpha_2)\}, \\ \varGamma_1^{**} = \{(\alpha_1, \alpha_2) : \alpha_1 = \alpha_1^{**}(\alpha_2)\}, \quad \varGamma_2 = \varGamma_2^* \cup \varGamma_2^{**}, \\ \varGamma_2^* = \{(\alpha_1, \alpha_2) : \alpha_2 = \alpha_2^*\}, \quad \varGamma_2^{**} = \{(\alpha_1, \alpha_2) : \alpha_2 = \alpha_2^{**}\}, \\ 0 \le \alpha_2^* < \alpha_2^{**} \le 2\pi . \end{array}$$

If the shell is closed in the circumferential direction, then $\alpha_2^* = 0, \alpha_2^{**} = 2\pi$, otherwise, one has the cylindrical panel. In the mixed variational principle (2.31), displacements and stresses are varied independently.

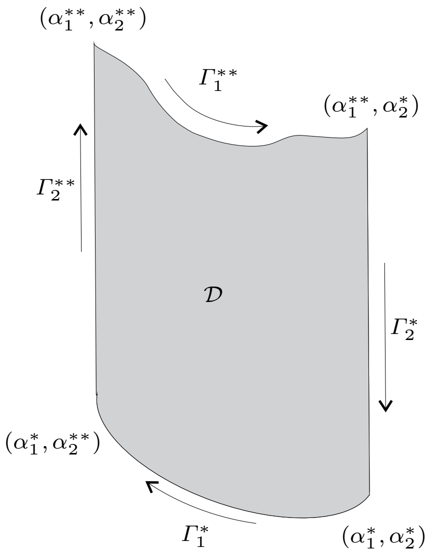

Fig. 2.4 Domain of the original surface and its bound. Path of integration.

The variation of the functional Π may be written in terms of the stress resultants, reduced moments and generalized strains $\hat{e}_{ij}$. Substituting Eqs. (2.5)-(2.9), (2.21)-(2.30) into (2.32) and introducing the generalized strains by (2.26), one obtains

$$\begin{aligned}\delta\Pi = \iint\limits_{\mathcal{D}} \Bigg\{ \sum_{i,j=1}^{2} \left(T_{ij}\delta\hat{e}_{ij} + \hat{M}_{ij}\delta\kappa_{ij} + \hat{L}_{ij}\delta\psi_{ij} \right) \\ + \sum_{i=1}^{2} Q_{0i}\delta\psi_i + \sum_{k=1}^{N} \int\limits_{\delta_{k-1}}^{\delta_k} \left(\bar{\epsilon}_3 - \mathbf{A}_3^{(k)}\bar{\sigma}_3 \right)^{\mathrm{T}} \delta\bar{\sigma}_3 \mathrm{d}z \Bigg\} \mathrm{d}\alpha_1 \mathrm{d}\alpha_2 .\end{aligned} \tag{2.34}$$

When deriving Eq. (2.34), we have neglected $k_{22}z$ $(k_{22}z \ll 1)$.

Let us apply the known generalized formula of partial integration

$$\iint\limits_{\mathcal{D}} F_1 \frac{\partial F_2}{\partial \alpha_1} \mathrm{d}\alpha_1 \mathrm{d}\alpha_2 = \int\limits_{\Gamma_1} F_1 F_2 \mathrm{d}\alpha_2 - \iint\limits_{\mathcal{D}} F_2 \frac{\partial F_1}{\partial \alpha_1} \mathrm{d}\alpha_1 \mathrm{d}\alpha_2 . \tag{2.35}$$

The standard variational procedure in (2.34) results in the following equation for the variation of the functional Π

$$\begin{aligned}\delta\Pi = &- \iint\limits_{\mathcal{D}} \Bigg\{ \sum_{i=1}^{2} \left(T_{1i,i} + T_{2i,2} \right) \delta\hat{u}_i + \sum_{i=1}^{2} \left(\hat{L}_{1i,1} + \hat{L}_{2i,2} - Q_{0i} \right) \delta\psi_i \\ &+ \sum_{i,j=1}^{2} \left[\hat{M}_{ij,ij} + \left(T_{ij} w_{,i} \right)_{,j} - k_{22} T_{22} \right] \delta w \Bigg\} \mathrm{d}\alpha_1 \mathrm{d}\alpha_2 \\ &+ \iint\limits_{\mathcal{D}} \Bigg\{ \sum_{k=1}^{N} \int\limits_{\delta_{k-1}}^{\delta_k} \left(\bar{\epsilon}_3 - \mathbf{A}_3^{(k)}\bar{\sigma}_3 \right)^{\mathrm{T}} \left[f_0(z)\delta\bar{\mu}^{(0)} + + f_k(z)\delta\bar{\mu}^{(k)} \right] \mathrm{d}z \Bigg\} \mathrm{d}\alpha_1 \mathrm{d}\alpha_2 \\ &+ \int\limits_{\Gamma_1} \Bigg[\sum_{i=1}^{2} \left(T_{i1}\delta\hat{u}_i + \hat{L}_{i1}\delta\psi_i \right) - \hat{M}_{11}\delta w_{,1} \\ &+ \left(\hat{M}_{11,\,1} + 2\hat{M}_{12,\,2} + T_{11} w_{,\,1} + T_{12} w_{,\,2} \right) \delta w \Bigg] \mathrm{d}\alpha_2 \\ &+ \int\limits_{\Gamma_2} \Bigg[\sum_{i=1}^{2} \left(T_{i2}\delta\hat{u}_i + \hat{L}_{i2}\delta\psi_i \right) - \hat{M}_{22}\delta w_{,2} \\ &+ \left(\hat{M}_{22,2} + 2\hat{M}_{12,2} + T_{12} w_{,1} + T_{22} w_{,2} \right) \delta w \Bigg] \mathrm{d}\alpha_1 ,\end{aligned} \tag{2.36}$$

where

$$\bar{\mu}^{(n)} = \left(\mu_1^{(n)},\, \mu_2^{(n)} \right)^{\mathrm{T}}, \quad n = 0, \ldots, k.$$

Let

$$\mathbf{q}_{\mathrm{s}} = \sum_{i=1}^{2} q_i \mathbf{e}_i + q_{\mathrm{n}} \mathbf{n} \tag{2.37}$$

be the vector of the external load acting on the unit area of the reference surface, where $q_i(\alpha_1, \alpha_2)$ are components of the tangential forces and $q_{\mathrm{n}}(\alpha_1, \alpha_2)$ is the normal load. Then the variation of the surface forces work will be

$$\delta A_1^* = \iint_{\mathcal{D}} \left(\sum_{i=1}^{2} q_i \delta u_1 + q_{\mathrm{n}} \delta w \right) \mathrm{d}\alpha_1 \mathrm{d}\alpha_2. \tag{2.38}$$

When turning to the generalized tangential displacements $\hat{u}_i$ by (2.26) and applying Eq. (2.35), it is written as follows

$$\begin{aligned} \delta A_1^* = & \iint_{\mathcal{D}} \left[\sum_{i=1}^{2} \left(q_i \delta \hat{u}_i + \hat{L}_{si} \delta \psi_i \right) + \hat{q}_{sn} \delta w \right] \mathrm{d}\alpha_1 \mathrm{d}\alpha_2 \\ & + \int_{\Gamma_1} \hat{Q}_{b1} \delta w \mathrm{d}\alpha_2 + \int_{\Gamma_2} \hat{Q}_{b2} \delta w \mathrm{d}\alpha_1, \end{aligned} \tag{2.39}$$

where

$$\hat{q}_{sn} = q_{\mathrm{n}} - \frac{1}{2} h c_{13} \sum_{i=1}^{2} q_{i,\,i} \tag{2.40}$$

is the reduced normal load which contains additional forces acting on the surface located at the distance $hc_{13}/2$ from the reference surface of the laminated shell,

$$\hat{L}_{si} = -\frac{1}{2} h c_{12} q_i, \quad i = 1, 2 \tag{2.41}$$

are the reduced moments generated by the components q_i and acting on the surface which is located at the distance $hc_{12}/2$ from the reference one, and

$$\hat{Q}_{bi} = \frac{1}{2} h c_{13} q_i \tag{2.42}$$

are the reduced shear boundary forces applied to the shell edges Γ_i at the distance $hc_{13}/2$ from the original surface. In contrast to Grigolyuk and Kulikov (1988), where $\hat{L}_{si} = \hat{Q}_{bi} = 0$ and $\hat{q}_{sn} = q_{\mathrm{n}}$, Eq. (2.39) takes into account the work of the tangential surface forces q_i.

Let us consider the boundary stress resultants T_{ij}^*, Q_i^* and M_{ij}^* $(i, j = 1, 2)$ acting on the shell counter $\Gamma_{\mathcal{D}} = \Gamma_1 \cup \Gamma_2$. Here, notations are the same as shown in Fig. 2.3, and the asterisk means that an appropriate force or moment is considered at the shell edge. Taking into account the additional degrees of freedom corresponding to the magnitudes ψ_i, we introduce also the generalized moments L_{ij}^* at the shell edges. The variation of the work of the external boundary forces may be presented in the form

$$\begin{aligned}\delta A_2^* = & \int\limits_{\Gamma_1} \Big[T_{11}^* \delta u_1 + T_{12}^* \delta u_2 + M_{11}^* \delta \theta_1 \\ & + \left(\frac{\partial M_{12}^*}{\partial \alpha_2} + Q_1^* \right) \delta w + L_{11}^* \delta \psi_1 + L_{12}^* \delta \psi_2 \Big] \,\mathrm{d}\alpha_2 \\ & + \int\limits_{\Gamma_2} \Big[T_{22}^* \delta u_2 + T_{21}^* \delta u_1 + M_{22}^* \delta \theta_2 \\ & + \left(\frac{\partial M_{21}^*}{\partial \alpha_1} + Q_2^* \right) \delta w + L_{22}^* \delta \psi_2 + L_{21}^* \delta \psi_1 \Big] \,\mathrm{d}\alpha_1 . \end{aligned} \tag{2.43}$$

Let us choose the path of integration in (2.43) as shown in Fig. 2.4. Then, introducing the generalized tangential displacements $\hat{u}_i$ by (2.26) and applying Eq. (2.35), one obtains the following equation

$$\begin{aligned}\delta A_2^* = & \int\limits_{\Gamma_1} \Big[T_{11}^* \delta \hat{u}_1 + T_{12}^* \delta \hat{u}_2 - \hat{M}_{11}^* \delta w_{,1} + \hat{L}_{11}^* \delta \psi_1 \\ & + \hat{L}_{12}^* \delta \psi_2 + \left(Q_1^* + \hat{M}_{12,2}^* \right) \delta w \Big] \,\mathrm{d}\alpha_2 \\ & + \int\limits_{\Gamma_2} \Big[T_{21}^* \delta \hat{u}_1 + T_{22}^* \delta \hat{u}_2 - \hat{M}_{22}^* \delta w_{,1} + \hat{L}_{22}^* \delta \psi_2 \\ & + \hat{L}_{21}^* \delta \psi_1 + \left(Q_2^* + \hat{M}_{21,1}^* \right) \delta w \Big] \,\mathrm{d}\alpha_1 + \frac{1}{2} h c_{13} \left[T_{12}^* \delta w \right]_\Gamma , \end{aligned} \tag{2.44}$$

where

$$\hat{L}_{ij}^* = L_{ij}^* - \frac{1}{2} h c_{12} T_{ij}^*, \quad \hat{M}_{ij}^* = M_{ij}^* - \frac{1}{2} h c_{13} T_{ij}^*, \tag{2.45}$$

and

$$\begin{aligned}\left[T_{12}^* \delta w \right]_\Gamma = & \; T_{12}^* \delta w |_{(\alpha_1^*, \alpha_2^{**})} - T_{12}^* \delta w |_{(\alpha_1^*, \alpha_2^*)} \\ & + T_{21}^* \delta w |_{(\alpha_1^{**}, \alpha_2^{**})} - T_{21}^* \delta w |_{(\alpha_1^*, \alpha_2^{**})} \\ & + T_{12}^* \delta w |_{(\alpha_1^{**}, \alpha_2^*)} - T_{12}^* \delta w |_{(\alpha_1^{**}, \alpha_2^{**})} \\ & + T_{21}^* \delta w |_{(\alpha_1^*, \alpha_2^*)} - T_{21}^* \delta w |_{(\alpha_1^{**}, \alpha_2^*)} . \end{aligned} \tag{2.46}$$

From Eqs. (2.6), (2.7), (2.24) it follows that $T_{12} = T_{21}$. Hence, one obtains that $T_{12}^* = T_{21}^*$. Then

$$\left[T_{12}^* \delta w \right]_\Gamma = 0. \tag{2.47}$$

2.1.7 Equilibrium Equations and Natural Boundary Conditions

Let us substitute Eqs. (2.36), (2.39), (2.44), (2.47) into the mixed variational principle (2.31). Taking into account the first hypothesis (2.2) coupling the transverse shear stresses σ_{i3} with the introduced additional functions $\mu_i^{(0)}(\alpha_1, \alpha_2)$, $\mu_i^{(k)}(\alpha_1, \alpha_2)$, we assume the displacements u_i, w, ψ_i and the functions $\mu_i^{(0)}, \mu_i^{(k)}$ to be independent. Equating coefficients of the variations of independent magnitudes u_i, w, ψ_i, $\mu_i^{(0)}, \mu_i^{(k)}$, we obtain:

- the desired five differential equations of equilibrium in terms of the reduced stress resultants

$$\begin{aligned} T_{1i,\,1} + T_{2i,\,2} &= -q_i, \\ \hat{L}_{1i,\,1} + \hat{L}_{2i,\,2} &= Q_{0i} - \hat{L}_{si}, \\ \hat{M}_{11,\,11} + 2\hat{M}_{12,\,12} + \hat{M}_{22,\,22} & \\ +w_{,\,11}T_{11} + 2w_{,\,12}T_{12} + w_{,\,22}T_{22} - k_{22}T_{22} &= -\hat{q}_{sn}, \end{aligned} \tag{2.48}$$

  with $i = 1, 2$,
- the equations coupling the transverse shear stresses with the shear strains

$$\sum_{k=1}^{N} \int_{\delta_{k-1}}^{\delta_k} \left(\bar{\epsilon}_3 - \mathbf{A}_3^{(k)}\bar{\sigma}_3\right) f_0(z)\mathrm{d}z = 0, \tag{2.49}$$

$$\int_{\delta_{k-1}}^{\delta_k} \left(\bar{\epsilon}_3 - \mathbf{A}_3^{(k)}\bar{\sigma}_3\right) f_k(z)\mathrm{d}z = 0 \tag{2.50}$$

  with $k = 1, 2, \ldots, N$, and
- the natural boundary conditions

$$\begin{aligned} &T_{i1} = T_{i1}^* \quad \text{or} \quad \hat{u}_i = 0, \\ &\hat{L}_{i1} = \hat{L}_{i1}^* \quad \text{or} \quad \psi_i = 0, \\ &\hat{M}_{11} = \hat{M}_{11}^* \quad \text{or} \quad w_{,\,1} = 0, \\ &\hat{M}_{11,1} + 2\hat{M}_{12,2} + T_{11}w_{,1} + T_{12}w_{,2} = Q_1^* + \hat{M}_{12,\,2}^* + \hat{Q}_{b1} \quad \text{or} \quad w = 0 \end{aligned} \tag{2.51}$$

  for the not necessary plane contours $\Gamma_1^*[\alpha_1 = \alpha_1^*(\alpha_2)], \Gamma_1^{**}[\alpha_1 = \alpha_1^{**}(\alpha_2)]$, and

$$\begin{aligned} &T_{i2} = T_{i2}^* \quad \text{or} \quad \hat{u}_i = 0, \\ &\hat{L}_{i2} = \hat{L}_{i2}^* \quad \text{or} \quad \psi_i = 0, \\ &\hat{M}_{22} = \hat{M}_{22}^* \quad \text{or} \quad w_{,\,2} = 0, \\ &\hat{M}_{22,2} + 2\hat{M}_{12,1} + T_{12}w_{,1} + T_{22}w_{,2} = Q_2^* + \hat{M}_{21,\,1}^* + \hat{Q}_{b2} \quad \text{or} \quad w = 0 \end{aligned} \tag{2.52}$$

  for the straight contours Γ_2^* $(\alpha_2 = \alpha_2^*)$ and Γ_2^{**} $(\alpha_2 = \alpha_2^{**})$.

The equilibrium equations (2.48) as well as the boundary conditions (2.51), (2.52) take into consideration the shear forces q_i applied to the reference surface and they are different from similar equations and boundary conditions derived by Grigolyuk and Kulikov (1988).

2.1.8 Transverse Shear Stresses and Their Resultants

We remind that because of the accepted hypothesis (2.2), the constitutive equations (2.15) are not satisfied. However, as seen from Eqs. (2.49) and (2.50), the constitutive equations for the transverse tangent stresses hold *integrally* for both the thickness of all laminated package with the weighting function $f_0(z)$ and the thickness of the k^{th} layer with the weighting function $f_k(z)$.

Equations (2.49), (2.50) allow us to couple the vector $\bar{\Psi}$ to the additional vectors $\bar{\mu}^{(0)}, \bar{\mu}^{(k)}$ (Grigolyuk and Kulikov, 1988). Indeed, the substitution of Eq. (2.2) for σ_{i3} and Eq. (2.6) for ϵ_{i3} into Eqs. (2.49), (2.50) results in the following system of $N+1$ algebraic equations for the vectors $\bar{\mu}^{(0)}, \bar{\mu}^{(k)}$

$$\sum_{k=1}^{N} \mathbf{A}_3^{(k)} \left(\lambda_k \bar{\mu}^{(0)} + \lambda_{k0} \bar{\mu}^{(k)} \right) = \sum_{k=1}^{N} \bar{\Psi},$$
$$\mathbf{A}_3^{(k)} \left(\lambda_{k0} \bar{\mu}^{(0)} + \lambda_{kk} \bar{\mu}^{(k)} \right) = \lambda_{k0} \bar{\Psi}, \tag{2.53}$$

where

$$\lambda_k = \int_{\delta_{k-1}}^{\delta_k} f_0^2(z) \mathrm{d}z, \qquad \lambda_{kn} = \int_{\delta_{k-1}}^{\delta_k} f_k(z) f_n(z) \mathrm{d}z, \qquad n = 0, k, \tag{2.54}$$

and

$$\mathbf{A}_3^{(k)} = \begin{pmatrix} G_k^{-1} & 0 \\ 0 & G_k^{-1} \end{pmatrix} \tag{2.55}$$

for the isotropic layers.

The solution of Eqs. (2.53) may be presented in the form

$$\mu_i^{(0)} = q_{44}^* \psi_i, \quad \mu_i^{(k)} = \frac{\lambda_{k0}}{\lambda_{kk}} \left(G_k \psi_i - \mu_i^{(0)} \right), \quad i = 1, 2; \; k = 1, 2, \ldots, N, \tag{2.56}$$

where

$$q_{44}^* = \frac{\sum_{k=1}^{N} \left(\lambda_k - \lambda_{k0}^2 \lambda_{kk}^{-1} \right)}{\sum_{k=1}^{N} \left(\lambda_k - \lambda_{k0}^2 \lambda_{kk}^{-1} \right) G_k^{-1}}. \tag{2.57}$$

Now, we can derive an equation for the generalized transverse stress resultants Q_{0i}. Substituting Eqs.(2.57) into (2.30), one obtains

$$Q_{0i} = q_{44} \, \psi_i, \tag{2.58}$$

where

$$q_{44} = \frac{\left[\sum\limits_{k=1}^{N}\left(\lambda_k - \dfrac{\lambda_{k0}^2}{\lambda_{kk}}\right)\right]^2}{\sum\limits_{k=1}^{N}\left(\lambda_k - \dfrac{\lambda_{k0}^2}{\lambda_{kk}}\right)G_k^{-1}} + \sum_{k=1}^{N}\frac{\lambda_{k0}^2}{\lambda_{kk}}G_k. \tag{2.59}$$

We shall call the magnitude $G = q_{44}/h$ as the reduced shear modulus for all package of the laminated shell.

2.1.9 Equations of Motion in Terms of Displacements

The system of five differential equations (2.48) together with Eqs. (2.27)-(2.29), (2.57) and Eqs. (2.6), (2.7), (2.26) for the stress resultants and strains, respectively, form the full system of equations for the five unknown generalized displacements $\hat{u}_i, w, \psi_i$. To derive these equations, it is convenient to write the stress resultants in terms of displacements.

The substitution of Eqs. (2.7), (2.26) into (2.27) and (2.29) results in the formulae for the in-plane stress resultants and reduced moments written in terms of the generalized displacements

$$\begin{aligned}
T_{ii} &= \frac{Eh}{1-\nu^2}\left[\hat{u}_{i,\,i} + \frac{1}{2}w_{,\,i}^2 + \nu\left(\hat{u}_{j,\,j} + \frac{1}{2}w_{,\,j}^2 + k_{ii}w\right) + k_{jj}w\right], \\
T_{ij} &= \frac{Eh}{2(1+\nu)}\left(\hat{u}_{i,\,j} + \hat{u}_{j,\,i} + w_{,\,i}w_{,\,j}\right), \\
\hat{M}_{ii} &= -\frac{Eh^3}{12(1-\nu^2)}\left[\eta_3(w_{,\,ii} + \nu w_{,\,jj}) - \eta_2(\psi_{i,\,i} + \nu\psi_{j,\,j})\right], \\
\hat{M}_{ij} &= -\frac{Eh^3}{12(1+\nu)}\left[\eta_3 w_{,\,ij} - \frac{1}{2}\eta_2(\psi_{i,\,j} + \psi_{j,\,i})\right], \\
\hat{L}_{ii} &= -\frac{Eh^3}{12(1-\nu^2)}\left[\eta_2(w_{,\,ii} + \nu w_{,\,jj}) - \eta_1(\psi_{i,\,i} + \nu\psi_{j,\,j})\right], \\
\hat{L}_{ij} &= -\frac{Eh^3}{12(1+\nu)}\left[\eta_2 w_{,\,ij} - \frac{1}{2}\eta_1(\psi_{i,\,j} + \psi_{j,\,i})\right],
\end{aligned} \tag{2.60}$$

where $i, j = 1, 2;\ i \neq j$. The generalized transverse stress resultants Q_{0i} are defined by (2.58), (2.59).

Introducing (2.60), (2.58), into Eqs. (2.48) yields the system of nonlinear differential equations in terms of the generalized displacements

$$\begin{aligned}
&\hat{u}_{1,11} + \frac{1-\nu}{2}\hat{u}_{1,22} + \frac{1+\nu}{2}\hat{u}_{2,12} + \nu k_{22} w_{,1} \\
&+ w_{,1}w_{,11} + \nu w_{,2}w_{,21} + \frac{1-\nu}{2}(w_{,1}w_{,22} + w_{,2}w_{,12}) = -\tilde{q}_1, \\
&\frac{1+\nu}{2}\hat{u}_{1,12} + \frac{1-\nu}{2}\hat{u}_{2,11} + \hat{u}_{2,22} + (k_{22}w)_{,2} \\
&+ \frac{1-\nu}{2}(w_{,2}w_{,11} + w_{,1}w_{,12}) + w_{,2}w_{,22} + \nu w_{,1}w_{,12} = -\tilde{q}_2, \\
&\eta_2 \triangle w_{,1} - \eta_1 \left(\psi_{1,11} + \frac{1+\nu}{2}\psi_{2,12} + \frac{1-\nu}{2}\psi_{1,22}\right) \\
&\qquad + \frac{12(1-\nu^2)}{Eh^3}\left(q_{44}\psi_1 + \frac{1}{2}hc_{12}q_1\right) = 0,
\end{aligned} \tag{2.61}$$

$$\begin{aligned}
&\eta_2 \triangle w_{,2} - \eta_1 \left(\psi_{2,22} + \frac{1+\nu}{2}\psi_{1,12} + \frac{1-\nu}{2}\psi_{2,11}\right) \\
&\qquad + \frac{12(1-\nu^2)}{Eh^3}\left(q_{44}\psi_2 + \frac{1}{2}hc_{12}q_2\right) = 0,
\end{aligned} \tag{2.62}$$

$$\begin{aligned}
&\frac{h^2}{12(1-\nu^2)}\triangle\left[\eta_3 \triangle w - \eta_2\left(\psi_{1,1} + \psi_{2,2}\right)\right] + \frac{k_{22}}{1-\nu^2}\left(\nu\hat{u}_{1,1} + \hat{u}_{2,2} + k_{22}w\right) \\
&- \frac{1}{1-\nu^2}\left\{ w_{,11}\left[\hat{u}_{1,1} + \nu(\hat{u}_{2,2} + k_{22}w) + \frac{1}{2}\left(w_{,1}^2 + \nu w_{,2}^2\right)\right] \right. \\
&+ w_{,22}\left[\nu\hat{u}_{1,1} + \hat{u}_{2,2} + k_{22}w + \frac{1}{2}\left(w_{,2}^2 + \nu w_{,1}^2\right)\right] \\
&\left. + (1-\nu)w_{1,12}(\hat{u}_{1,2} + \hat{u}_{2,1} + w_{,1}w_{,2}) - \frac{1}{2}k_{22}\left(w_{,2}^2 + \nu w_{,1}^2\right)\right\} = \tilde{q}_{\mathrm{n}},
\end{aligned} \tag{2.63}$$

where

$$\triangle = \frac{\partial^2}{\partial\alpha_1^2} + \frac{\partial^2}{\partial\alpha_2^2}$$

is the Laplace operator, and

$$\tilde{q}_i = \frac{(1-\nu^2)q_i}{Eh}, \quad \tilde{q}_{\mathrm{n}} = \frac{1}{Eh}\left(q_{\mathrm{n}} - \frac{1}{2}hc_{13}\sum_{i=1}^{2} q_{i,i}\right). \tag{2.64}$$

The static balance equations (2.61)-(2.64) are in the usual way transformed into equations describing the shell motion. When neglecting the rotary inertia effects, in accordance with d'Alembert principle one assumes

$$\begin{aligned}
\tilde{q}_i &= \frac{(1-\nu^2)}{Eh}\left(q_i - \sum_{k=1}^{N}\rho_k h_k \frac{\partial^2 \hat{u}_i}{\partial t^2}\right), \\
\tilde{q}_{\mathrm{n}} &= \frac{1}{Eh}\left(q_{\mathrm{n}} - \frac{1}{2}hc_{13}\sum_{i=1}^{2} q_{i,i} - \sum_{k=1}^{N}\rho_k h_k \frac{\partial^2 w}{\partial t^2}\right),
\end{aligned} \tag{2.65}$$

where ρ_k is the specific density of a material of the k^{th} layer, and t is time. If $q_i = q_{\rm n} = 0$, and $T^*_{ij}, L^*_{ij}, M^*_{ij}$ are specified static stress resultants on the shell edges, then Eqs. (2.61)-(2.64), together with (2.65), describe free vibrations.

2.1.10 In-plane Stress State Equations

Let us introduce the index of variation ι of the stress-strain state as

$$\max\{|Z_{,1}|,\ |Z_{,2}|\} \sim h_*^{-\iota} Z, \tag{2.66}$$

where $h_* = h/R$ is the dimensional thickness which is assumed as a small parameter, R is the characteristic dimension of the shell, and Z is any unknown function which determines this state. Here and below, the symbol $\sim$ means that two quantities have the same asymptotic orders at $h_* \to 0$ (s. the definition in Chapt. 6).

Depending on a value of ι and orders of all unknown functions in Eqs. (2.48) or (2.61)-(2.63), one can deduce simplified equations corresponding to different stress-strain state of a shell. The classification of the characteristic stress-strain states of a thin single layer isotropic shell has been proposed by Gol'denveizer (1961) and Novozhilov (1970).

In this subsection, we consider the simplest state called *the membrane* (*momentless*) stress-strain state[1]. This state is characterized by slow variation of all unknown functions ($\iota = 0$) and displacements $\hat{u}_i, w, R\psi_i$ being small quantities of the order Rh_*. The governing equations for this state can be derived from Eqs. (2.48) or (2.61)-(2.63). When omitting nonlinear terms in (2.48) and introducing the inertial terms, then the dynamic in-plane stress resultants satisfy the following system of equations

$$\begin{aligned} \frac{\partial T_{11}}{\partial \alpha_1} + \frac{\partial T_{21}}{\partial \alpha_2} &= -q_1(\alpha_1, \alpha_2, t) + \rho_0 h \frac{\partial^2 \hat{u}_1}{\partial t^2}, \\ \frac{\partial T_{12}}{\partial \alpha_1} + \frac{\partial T_{22}}{\partial \alpha_2} &= -q_2(\alpha_1, \alpha_2, t) + \rho_0 h \frac{\partial^2 \hat{u}_2}{\partial t^2}, \\ k_{22} T_{22} &= \hat{q}_{sn}(\alpha_1, \alpha_2, t) - \rho_0 h \frac{\partial^2 w}{\partial t^2}, \end{aligned} \tag{2.67}$$

where

$$\rho_0 = \sum_{k=1}^{N} \rho_k \xi_k, \tag{2.68}$$

and ξ_k is computed by (2.25).

Equations (2.67) may be used to specify the dynamic stress-strain state if q_i and $\hat{q}_{sn}$ are slowly varying functions of time t and coordinates α_i. They may be rewritten in terms of the generalized displacements

[1] The term *membrane stress-strain state* is established in the literature. Since membranes cannot be affected by compression forces it is better to use *in-plane stress-strain state*.

$$\begin{gathered}
\hat{u}_{1,\,11}+\frac{1-\nu}{2}\hat{u}_{1,\,22}+\frac{1+\nu}{2}\hat{u}_{2,\,12}+\nu k_{22}w_{,\,1}=-\tilde{q}_{1},\\
\frac{1+\nu}{2}\hat{u}_{1,\,12}+\frac{1-\nu}{2}\hat{u}_{2,\,11}+\hat{u}_{2,\,22}+(k_{22}w)_{,\,2}=-\tilde{q}_{2},\\
\frac{k_{22}}{1-\nu^{2}}\left(\nu\hat{u}_{1,\,1}+\hat{u}_{2,\,2}+k_{22}w\right)=\tilde{q}_{\mathrm{n}}.
\end{gathered}\tag{2.69}$$

The corresponding boundary conditions are defined for the in-plane stress resultants T_{ij} or displacements $\hat{u}_i$.

2.1.11 Technical Theory Equations

Equations (2.61)-(2.63), together with an appropriate variant of the boundary conditions (2.51) or (2.52), turn out to be complicated for the analysis of both static and dynamic stress-strain state. However, they may be significantly simplified under some additional assumptions.

We will consider here the stress state which is characterized by the index of variation $\iota = 1/2$ and the following estimates:

$$w \sim h_* R, \quad k_{22} \sim R^{-1}, \quad u_i \ll w. \tag{2.70}$$

It is obvious that $\hat{u}_i \ll w$ also. Let

$$\max\{\hat{u}_i\} \sim h_*^{\zeta_u} R, \quad \max\{\psi_i\} \sim h_*^{\zeta_\psi}, \quad G \sim h_*^{\zeta_G} E, \tag{2.71}$$

where ζ_u, ζ_ψ are the indexes of intensity of the quantities $\hat{u}_i, \psi_i$, respectively, and $h_*^{\zeta_G}$ is the order of the reduced shear modulus G with regard to the reduced Young's modulus E. If any layer is viscoelastic, then the last estimate in (2.71) is replaced by $G_{\mathrm{r}} \sim h_*^{\zeta_G} E_{\mathrm{r}}$, where $E_{\mathrm{r}} = \Re E, G_{\mathrm{r}} = \Re G$ are the real parts of moduli E, G. Then, analyzing the orders of all terms in Eqs. (2.61)-(2.63), we find

$$\zeta_u = 3/2, \quad \zeta_\psi = 1/2, \quad \zeta_G = 1. \tag{2.72}$$

The stress-strain state characterized by the above indexes of variation and intensity is called the nonlinear *combined* stress state (Tovstik and Smirnov, 2001). For this state all terms in Eqs. (2.61)-(2.63), including non-linear ones, has the same order. If $w \ll h_* R$, then non-linear summands in the governing equations may be omitted.

Let $q_i = 0$ and the inertia forces in the tangential directions are very small. Then Eqs. (2.61) or (2.48) become homogeneous

$$T_{1i,\,1} + T_{2i,\,2} = 0. \tag{2.73}$$

They are identically satisfied by the following functions

$$T_{ij} = \delta_{ij}\triangle F - F_{,ij}, \tag{2.74}$$

where δ_{ij} is the Kronecker delta, and F is the unknown stress function.

To couple the introduced stress function with the unknown displacements, we apply the strain compatibility condition. With this purpose in mind, we will write down the correlations, following from Eqs. (2.26) and (2.7), and linking the generalized strains and displacements

$$\begin{aligned} \hat{e}_{11} &= \hat{u}_{1,1} + \frac{1}{2}\left(w_{,1}\right)^2, \\ \hat{e}_{22} &= \hat{u}_{2,22} + k_{22}w + \frac{1}{2}\left(w_{,2}\right)^2, \\ \hat{e}_{12} &= \frac{1}{2}\left(\hat{u}_{1,2} + \hat{u}_{2,1} + w_{,1}w_{,2}\right). \end{aligned} \tag{2.75}$$

Eliminating $\hat{u}_i$, one obtains the strain compatibility equation

$$\hat{e}_{11,22} - 2\hat{e}_{12,12} + \hat{e}_{22,11} = k_{22}w_{,11} + \left(w_{,12}\right)^2 - w_{,11}w_{,22}. \tag{2.76}$$

Expressing the generalized strains $\hat{e}_{ij}$ by the stress function F by Eq. (2.27) and introducing them into (2.76) yield the following equation

$$\triangle^2 F - Eh\left[k_{22}w_{,11} + \left(w_{,12}\right)^2 - w_{,11}w_{,22}\right] = 0. \tag{2.77}$$

Considering Eqs. (2.62) and following Grigolyuk and Kulikov (1988), we introduce new functions a and ϕ so that

$$\psi_1 = a_{,1} + \phi_{,2}, \quad \psi_2 = a_{,2} - \phi_{,1}. \tag{2.78}$$

The substitution of (2.78) into (2.62) gives

$$\begin{aligned} \frac{Eh^3}{12(1-\nu^2)}\triangle(\eta_1 a - \eta_2 w)_{,1} + \frac{Eh^3}{24(1+\nu^2)}\eta_1\triangle\phi_{,2} = q_{44}(a_{,1} + \phi_{,2}), \\ \frac{Eh^3}{12(1-\nu^2)}\triangle(\eta_1 a - \eta_2 w)_{,2} - \frac{Eh^3}{24(1+\nu^2)}\eta_1\triangle\phi_{,1} = q_{44}(a_{,2} - \phi_{,1}). \end{aligned} \tag{2.79}$$

It may be seen that these equations are identically satisfied if

$$\frac{Eh^3}{12(1-\nu^2)}\triangle(\eta_1 a - \eta_2 w) = q_{44}a, \tag{2.80}$$

$$\frac{Eh^3}{24(1+\nu)}\eta_1\triangle\phi = q_{44}\phi \tag{2.81}$$

are assumed.

Let us introduce the displacement χ as (Grigolyuk and Kulikov, 1988)

$$w = \left(1 - \frac{h^2}{\beta}\triangle\right)\chi, \tag{2.82}$$

$$a = -\frac{\eta_2}{\eta_1}\frac{h^2}{\beta}\triangle\chi \tag{2.83}$$

and substitute them into Eq. (2.80). It can be seen that Eq. (2.80) is identically satisfied if and only if

$$\beta = \frac{12(1-\nu^2)q_{44}}{Eh\eta_1}. \tag{2.84}$$

Then Eq. (2.81) can be rewritten as

$$\frac{1-\nu}{2}\frac{h^2}{\beta}\triangle\phi = \phi. \tag{2.85}$$

Consider the last equation of equilibrium, Eq. (2.63) may be rewritten as

$$\begin{gathered}\frac{Eh^3}{12(1-\nu^2)}\triangle\left[\eta_3\triangle w - \eta_2\left(\psi_{1,1} + \psi_{2,2}\right)\right] \\ -w_{,11}T_{11} - 2w_{,12}T_{12} - w_{,22}T_{22} + k_{22}T_{22} = q_{\mathrm{n}} - \sum_{k=1}^{N}\rho_k h_k\frac{\partial^2 w}{\partial t^2}.\end{gathered} \tag{2.86}$$

The substitution of Eqs. (2.74), (2.78), (2.82) and (2.83) into (2.86) after some transforms results in the following equation

$$D\left(1 - \frac{\theta h^2}{\beta}\triangle\right)\triangle^2\chi - F_{,22}w_{,11} + 2F_{,12}w_{,12} + F_{,11}(k_{22} - w_{,22}) = q_{\mathrm{n}} - \rho_0 h\frac{\partial^2 w}{\partial t^2}, \tag{2.87}$$

where

$$D = \frac{Eh^3}{12(1-\nu^2)}\eta_3 \tag{2.88}$$

is the reduced bending stiffness of the laminated cylindrical shell, and

$$\theta = 1 - \frac{\eta_2^2}{\eta_1\eta_3}. \tag{2.89}$$

Calculations performed by Grigolyuk and Kulikov (1988) have shown that θ is a small parameter. So, for a single layer shell $\theta = 1/85$.

The simplified system of governing equations (2.77), (2.82), (2.85) and (2.87) was at first derived by Grigolyuk and Kulikov (1988). The limiting process at $G \to \infty$ (or $\beta^{-1} \to 0$) implies

$$\chi \to w, \quad a \to 0,$$

and this system degenerates into that of nonlinear equations of the technical theory of thin isotropic shells based on the Kirchhoff-Love hypotheses

$$D\triangle^2 w - F_{,22}w_{,11} + 2F_{,12}w_{,12} + F_{,11}(k_{22} - w_{,22}) = q_{\mathrm{n}} - \rho_0 h\frac{\partial^2 w}{\partial t^2},$$
$$\triangle^2 F - k_{22}Ehw_{,11} + (w_{,12})^2 - w_{,11}w_{,22} = 0.$$

The linearization of Eqs. (2.77) and (2.87), with Eq. (2.82) taken into account, results in the following coupled equations

$$\begin{aligned} &D\left(1 - \frac{\theta h^2}{\beta}\triangle\right)\triangle^2\chi - k_{22}F_{,11} = q_{\mathrm{n}} - \rho_0 h\frac{\partial^2}{\partial t^2}\left(1 - \frac{h^2}{\beta}\triangle\right)\chi, \\ &\triangle^2 F - Eh\left[k_{22}\left(1 - \frac{h^2}{\beta}\triangle\right)\chi_{,11}\right] = 0. \end{aligned} \tag{2.90}$$

which will be generally used below for studying small forced and free vibrations of laminated cylindrical shells. When omitting the terms proportional to β^{-1}, one arrives at the well-known Mushtari-Donnell-Vlasov type equations (Mushtari and Galimov, 1961; Donnell, 1976; Wlassow, 1958).

2.1.12 Error of Governing Equations

The determination of an exact error of the developed single layer model for a multilayered shell is a complicated problem which is not considered here. Below, to estimate approximately its error, we shall compare eigenvalues of some boundary-value problems on buckling and vibrations with results obtained by using the 3D finite-element simulation. In this subsection, we aim only to give some *asymptotic* estimations of errors of the governing equations based on the generalized Timoshenko hypotheses.

It is known that the error δ_{e} of the Kirchhoff-Love hypotheses has the order $\delta_{\mathrm{e}} \sim h_*$. It may be expected that accepted here the generalized Timoshenko hypotheses improves an accuracy of the governing equations and results in the error $\delta_{\mathrm{e}} \sim h_*^q$, where $q \geq 1$. However, as has been shown by Gol'denveizer (1961) and Koiter (1966), the index of variation ι of an expected solution may give the conclusive contribution in the estimation of an error. If $\iota < 1$, then in the framework of the Kirchhoff-Love hypotheses, this estimation is defined as

$$\delta_{\mathrm{e}} \sim \max\left\{h_*, h_*^{2-2\iota}\right\}.$$

For the governing equations (2.61)-(2.63) based on the generalized Timoshenko hypotheses, one has

$$\delta_{\mathrm{e}} \sim \max\left\{h_*^q, h_*^{2-2\iota}\right\}, \tag{2.91}$$

where $q \geq 1$. The peculiarity of Eqs. (2.61)-(2.63) and Eqs. (2.90) is that due to shears they have solutions with very high index of variation. So, for an isotropic and homogeneous shell with Young's and shear moduli E, G having the same asymptotic order ($E \sim G$), additional integrals taking into account shear have the index of variation $\iota = 1$. Then $\delta_{\mathrm{e}} \sim 1$ and Eqs. (2.61)-(2.63) as well as Eqs. (2.90) become asymptotically incorrect. But if $G \sim h_*^{\zeta_G} E$, where $\zeta_G > 0$, then $\iota = 1 - \zeta_G/2 < 1$.

Now, consider Eqs. (2.90) which are analogous to the well-known Mushtari-Donnell-Vlasov type equations (Mushtari and Galimov, 1961; Donnell, 1976; Wlassow, 1958). They were obtained after significant simplifications which introduced the error of order $h_*^{2\iota}$. It is seen that the error of this equations has the order

$$\delta_{\mathrm{e}} \sim \max\left\{h_*^{2\iota}, h_*^{2-2\iota}\right\}. \tag{2.92}$$

We remind that Eqs. (2.90) were derived under assumptions that $\iota = 1/2, \zeta_G = 1$. Hence, for solutions with the index $\iota = 1/2$, one obtains the error $\delta_{\mathrm{e}} \sim h_*$.

Equations (2.90) can be also used to describe the *semi-momentless* dynamic stress state characterized by the index of variation $\iota = 1/4$ for a shear pliable shell with $\zeta_G \geq 1$. However, for solutions having the index of variation $\iota = 1/4$ (at $\zeta_G = 3/2$), the error increases and reaches the order $\delta_{\mathrm{e}} \sim h_*^{1/2}$.

2.1.13 Displacement and Stress Function Boundary Conditions

If a problem (on buckling or vibration) is solved on the bases of the technical shell theory, the boundary conditions (2.51), (2.52) should be rewritten in terms of the displacements, stress and shear functions, χ, F and ϕ. Consider possible variants of the boundary conditions (2.51) at $\alpha_1 = \alpha_1^*$

1. The generalized displacements are bounded in the tangential directions

$$\hat{u}_1 = 0, \quad \hat{u}_2 = 0. \tag{2.93}$$

This variant is more difficult because the generalized displacements $\hat{u}_i$ are not expressed in the explicit form of χ, F and ϕ. However, Eqs. (2.7), (2.26), (2.27), (2.74), (2.78), (2.82) and (2.83) lead to the following system of differential equations for $\hat{u}_i$

$$\begin{aligned}
\hat{u}_{1,1} &= \frac{1}{Eh}(F_{,22} - \nu F_{,11}) + \frac{1}{2}hc_{13}\left(1 - \frac{h^2}{\beta}\triangle\right)\chi_{,11} \\
&\quad + \frac{1}{2}hc_{12}\left(\frac{\eta_2}{\eta_1}\frac{h^2}{\beta}\triangle\chi_{,11} - \phi_{,12}\right), \\
\hat{u}_{2,2} &= \frac{1}{Eh}(F_{,11} - \nu F_{,22}) + \frac{1}{2}hc_{13}\left(1 - \frac{h^2}{\beta}\triangle\right)\chi_{,22} \\
&\quad + \frac{1}{2}hc_{12}\left(\frac{\eta_2}{\eta_1}\frac{h^2}{\beta}\triangle\chi_{,22} - \phi_{,12}\right) - k_{22}\left(1 - \frac{h^2}{\beta}\triangle\right)\chi, \\
\hat{u}_{1,2} + \hat{u}_{2,1} &= -\frac{2(1+\nu)}{Eh}F_{,12} + hc_{13}\left(1 - \frac{h^2}{\beta}\triangle\right)\chi_{,12} \\
&\quad + \frac{1}{2}hc_{12}\left(\frac{2\eta_2}{\eta_1}\frac{h^2}{\beta}\triangle\chi_{,12} + \phi_{,11} - \phi_{,22}\right).
\end{aligned} \tag{2.94}$$

When solving Eqs. (2.94), we can satisfy conditions (2.93).

2. The edge is prestressed in the tangential directions

$$T_{11} = T_{11}^*, \quad T_{21} = T_{21}^*. \tag{2.95}$$

These conditions are equivalent to the following ones

$$F_{,22} = T_{11}^*, \quad F_{,21} = -T_{21}^*. \tag{2.96}$$

3. The conditions

$$\psi_1 = \psi_2 = 0 \tag{2.97}$$

mean that the shear in the axial and circumferential directions, respectively, are absent. They result in the equations

$$-\frac{\theta_2}{\theta_1}\frac{h^2}{\beta}\triangle\chi_{,1} + \phi_{,2} = 0, \quad \frac{\theta_2}{\theta_1}\frac{h^2}{\beta}\triangle\chi_{,2} + \phi_{,1} = 0. \tag{2.98}$$

4. The generalized bending and twisting couples are specified at the edge

$$\hat{L}_{11} = \hat{L}_{11}^*, \quad \hat{L}_{21} = \hat{L}_{21}^*. \tag{2.99}$$

These conditions are rewritten as follows

$$\begin{aligned} \chi_{,11} + \nu\chi_{,22} - (1-\nu)\phi_{,12} &= -\frac{\hat{L}_{11}^*}{D\gamma}, \\ \chi_{,12} - \frac{1}{2}(\phi_{,22} - \phi_{,11}) &= -\frac{\hat{L}_{21}^*}{D\gamma(1-\nu)}. \end{aligned} \tag{2.100}$$

5. The condition

$$w_{,1} = 0 \tag{2.101}$$

means that the edge does not rotate about the vector $\boldsymbol{e}_2$. It is reduced to the equation

$$\left(1 - \frac{h^2}{\beta}\triangle\right)\chi_{,1} = 0. \tag{2.102}$$

6. The generalized bending moment is specified

$$\hat{M}_{11} = \hat{M}_{11}^*. \tag{2.103}$$

This condition may be rewritten as

$$-\left(1 - \frac{\theta h^2}{\beta}\triangle\right)(\chi_{,11} + \nu\chi_{,22}) + (1-\nu)(1-\theta)\phi_{,12} = \frac{\hat{M}_{11}^*}{D}. \tag{2.104}$$

7. The condition $w = 0$ is equivalent to

$$\left(1-\frac{h^2}{\beta}\triangle\right)\chi=0. \tag{2.105}$$

8. The shear force in the $\boldsymbol{n}$-direction is specified

$$\hat{M}_{11,\,1}+2\hat{M}_{12,\,2}+T_{11}w_{,\,1}+T_{12}w_{,\,2}=Q_1^*+\hat{M}^*_{12,\,2}. \tag{2.106}$$

The substitution of Eqs. (2.60) for $\hat{M}_{1i}$ into Eq. (2.123), with Eqs. (2.7), (2.74), (2.78), (2.82) and (2.83) taken into account, results in the following condition at $\alpha_1 = \alpha_1^*$

$$-\left(1-\frac{\theta h^2}{\beta}\triangle\right)[\chi_{,\,111}+(2-\nu)\chi_{,\,122}]+(1-\nu)(1-\theta)\phi_{,\,222}$$
$$+\frac{1}{D}\left[F_{,\,22}\left(1-\frac{h^2}{\beta}\triangle\right)\chi_{,\,1}-F_{,\,12}\left(1-\frac{h^2}{\beta}\triangle\right)\chi_{,\,2}\right]=\frac{1}{D}\left(Q_1^*+\hat{M}^*_{12,\,2}\right). \tag{2.107}$$

If

$$Q_1^*+\hat{M}^*_{12,\,2}=0, \tag{2.108}$$

then the edge is free for displacements in the $\boldsymbol{n}$-direction, that is $w\neq 0$.

The natural boundary conditions listed above may be classified into four groups:

a) (2.93) and (2.96);
b) (2.98) and (2.100);
c) (2.102) and (2.104);
d) (2.105) and (2.107).

Within the range of each group, different boundary conditions are simultaneously not satisfied. For instance, if the homogeneous conditions (2.96) hold, then the edge $\alpha_1 = \alpha_1^*$ is free for the in-plane displacements, hence, $\hat{u}_i \neq 0$. And if conditions (2.100) are valid, then the shell is free for the shear in the α_i-direction, i.e., $\psi_i \neq 0$.

The list of boundary conditions given above is not complete. It does not contain the superposition of conditions from a fixed group from a)-d). For example, the equation

$$F_{,\,22}=k_{sp}\hat{u}_1 \quad \text{at} \quad \alpha_1=\alpha_1^*, \tag{2.109}$$

where, k_{sp} is the spring constant of a surrounding medium in the axial direction, represents the condition of elastic support of the edge in the $\boldsymbol{e}_1$-direction.

Some of the boundary conditions listed above are expressed by too complicated equations. However, in some cases their combinations result in simple equations:

1. The edge $\alpha_1 = \alpha_1^*$ is simply supported, but there is the infinite rigidity diaphragm inhibiting shear along the edge plane

$$w=\hat{M}_{11}=\hat{L}_{11}=\psi_2=0. \tag{2.110}$$

In terms of the displacement, stress and shear functions, these conditions are represented by Eqs. (2.105), (2.103), (2.100) and (2.99), respectively, and after calculations may be reduced to the following conditions

$$\chi = \varDelta\chi = \varDelta^2\chi = \frac{\partial \phi}{\partial \alpha_1} = 0. \tag{2.111}$$

2. The edge $\alpha_1 = \alpha_1^*$ is simply supported, and the diaphragm is absent

$$w = \hat{M}_{11} = \hat{L}_{11} = \hat{L}_{12} = 0. \tag{2.112}$$

This combination of the boundary conditions is rewritten as follows

$$\begin{gathered}
\left(1 - \frac{h^2}{\beta}\varDelta\right)\chi = 0, \quad \frac{\partial^2}{\partial \alpha_1^2}\left(1 - \frac{h^2}{\beta}\varDelta\right)\chi = 0, \\
\left(\frac{\partial^2}{\partial \alpha_1^2} + \nu\frac{\partial^2}{\partial \alpha_2^2}\right)\chi - (1-\nu)\frac{\partial^2 \phi}{\partial \alpha_1 \alpha_2} = 0, \\
2\frac{\partial^2 \chi}{\partial \alpha_1 \partial \alpha_2} + \frac{\partial^2 \phi}{\partial \alpha_1^2} - \frac{\partial^2 \phi}{\partial \alpha_2^2} = 0.
\end{gathered} \tag{2.113}$$

3. The edge $\alpha_1 = \alpha_1^*$ is clamped, and there is the infinite rigidity diaphragm inhibiting shear along the edge plane

$$w = \frac{\partial w}{\partial \alpha_1} = \psi_1 = \psi_2 = 0 \tag{2.114}$$

or

$$\begin{gathered}
\left(1 - \frac{h^2}{\beta}\varDelta\right)\chi = 0, \quad \frac{\partial}{\partial \alpha_1}\left(1 - \frac{h^2}{\beta}\varDelta\right)\chi = 0, \\
\frac{\partial \chi}{\partial \alpha_1} - \frac{\partial \phi}{\partial \alpha_2} = 0, \quad \frac{\partial \chi}{\partial \alpha_2} + \frac{\partial \phi}{\partial \alpha_1} = 0.
\end{gathered} \tag{2.115}$$

4. The edge $\alpha_1 = \alpha_1^*$ is clamped, and the diaphragm is absent

$$w = \frac{\partial w}{\partial \alpha_1} = \psi_1 = \hat{L}_{12} = 0 \tag{2.116}$$

or

$$\left(1 - \frac{h^2}{\beta}\varDelta\right)\chi = 0, \quad \frac{\partial \chi}{\partial \alpha_1} = \frac{\partial}{\partial \alpha_1}(\varDelta\chi) = \phi = 0. \tag{2.117}$$

It is seen that each variant from (2.111), (2.113), (2.115) or (2.117) is incomplete because it does not contain conditions for the generalized in-plane displacements $\hat{u}_i$ or stress resultants T_{i1}. For example, the conditions of free support, $T_{11} = \hat{e}_{22} = 0$, results in the additional conditions for the stress function (Grigolyuk and Kulikov, 1988)

$$F = \triangle F = 0 \quad \text{at} \quad \alpha_1 = \alpha_1^*. \tag{2.118}$$

In what follows, the boundary conditions (2.111) and (2.113) supplemented by Eqs. (2.118) will be considered as the basic ones. To study the main stress state of a shell with clamped edges, it will be sufficient to satisfy conditions (2.115) or (2.117) without considering the additional conditions for the in-plane displacements and/or the in-plane stress resultants.

2.1.14 Edge Effect Equations

In many cases the shell stress-strain state may be considered as a superposition of the main stress-strain stateand edge effects (Gol'denveizer, 1961). For a thin isotropic cylindrical shell the edge effect has the index of variation $\iota_1 = 1/2$ in the neighbourhood of an edge (e.g., $\alpha_1 = \alpha_1^*$) in the direction orthogonal to the edge and a small index of variation ι_2 in the circumferential direction. All magnitudes corresponding to this stress state are quickly decreasing functions as $|\alpha_1 - \alpha_1^*| \to \infty$.

In the theory of laminated shells based on the generalized Timoshenko hypotheses (2.2)-(2.4), the edge effect equations are derived in the same way as in the Kirchhoff-Love hypotheses based theory (Mikhasev, 2016). Let us consider the linearized Eqs. (2.61)-(2.63) and assume the following asymptotic estimates

$$\begin{aligned}
&w \sim h_* R, \quad \hat{u}_1 \sim h_*^{3/2} R, \quad \hat{u}_2 \sim h_*^{7/4} R, \quad \psi_i \sim h_*^{1/2},\\
&\left|\frac{\partial Z}{\partial \alpha_1}\right| \sim h_*^{-\iota_1} Z, \quad \left|\frac{\partial Z}{\partial \alpha_2}\right| \sim h_*^{-\iota_2} Z, \quad G \sim h_* E, \quad \iota_1 = 1/2, \quad \iota_2 \le 1/4,\\
&|q_1| \sim \frac{E}{1-\nu^2} h_*^{3/2}, \quad |q_2| \sim \frac{E}{1-\nu^2} h_*^{7/4}, \quad |q_{\rm n}| \sim E h_*^2 \quad \text{as} \quad h_* \to 0
\end{aligned} \tag{2.119}$$

which satisfy the above mentioned assumptions (2.70)-(2.72) for the *combined* stress state. In Eqs. (2.119), Z denotes any from the functions $\hat{u}_i, w, \psi_i$.

In each equation of system (2.61)-(2.63), we consider the main terms having the same order as $h_* \to 0$. In the first and second equations (2.61), the main summands have the orders $h_*^{1/2} R^{-1}$ and $h_*^{3/4} R^{-1}$, respectively. When taking these terms into account and omitting remaining ones, then Eqs. (2.61) are reduced to the differential equations

$$\frac{\partial^2 \hat{u}_1}{\partial \alpha_1^2} + \nu k_{22}(\alpha_2) \frac{\partial w}{\partial \alpha_1} = -\tilde{q}_1, \tag{2.120}$$

$$\frac{1+\nu}{2} \frac{\partial^2 \hat{u}_1}{\partial \alpha_1 \partial \alpha_2} + \frac{1-\nu}{2} \frac{\partial^2 \hat{u}_2}{\partial \alpha_1^2} + \frac{\partial}{\alpha_2} \left[k_{22}(\alpha_2) w\right] = -\tilde{q}_2. \tag{2.121}$$

In both Eqs. (2.62), the main terms have the order $h_*^{-1/2} R^{-2}$ and generate the following equations

$$\frac{\partial^2 \psi_2}{\partial \alpha_1^2} = \frac{2\beta}{(1-\nu) h^2} \psi_2, \tag{2.122}$$

$$\eta_2 \frac{\partial^3 w}{\partial \alpha_1^3} - \eta_1 \frac{\partial^2 \psi_1}{\partial \alpha_1^2} + \frac{\beta \eta_1}{h^2} \psi_1 = 0. \tag{2.123}$$

Writing these equations down, we have taken into account Eqs. (2.54), (2.59) and assumed the following estimation

$$q_{44} \sim h_* R G \tag{2.124}$$

as well. Finally, in Eq. (2.63), the main terms of the order $h_* R^{-1}$ give

$$\frac{h^2}{12(1-\nu^2)}\left(\eta_3 \frac{\partial^4 w}{\partial \alpha_1^4} - \eta_2 \frac{\partial^3 \psi_1}{\partial \alpha_1^3}\right) + \frac{k_{22}(\alpha_2)\nu}{1-\nu^2}\frac{\partial \hat{u}_1}{\partial \alpha_1} + \frac{k_{22}^2(\alpha_2)}{1-\nu^2} w = \tilde{q}_{\mathrm{n}}. \tag{2.125}$$

As seen, Eq. (2.122) for ψ_2 is independent of the others and the same as Eq. (2.85) for ϕ.

Let the surface load intensity be not high and its components satisfy the following inequalities

$$|q_1| \ll \frac{E}{1-\nu^2} h_*^{3/2}, \quad |q_2| \ll \frac{E}{1-\nu^2} h_*^{7/4}, \quad |q_{\mathrm{n}}| \ll E h_*^2. \tag{2.126}$$

Then $\tilde{q}_i, q_{\mathrm{n}}$ may be omitted,

$$\tilde{q}_{\mathrm{n}} = -\frac{\rho_0}{E}\frac{\partial^2 w}{\partial t^2},$$

and Eqs. (2.120), (2.121) and (2.124) degenerate into homogeneous ones which describe the simple edge effect.

From all solutions of the homogeneous equations (2.120)-(2.124), one needs to choose such integrals which satisfy conditions

$$\hat{u}_i, \psi_i, w \to 0 \quad \text{at} \quad |\alpha_1 - \alpha_1^*| \to \infty. \tag{2.127}$$

Fulfilling some transforms with the homogeneous equations (2.120), (2.123), (2.124), with condition (2.127) in mind, one obtains the basic equation of the dynamic edge effect

$$\frac{h^2\eta_3}{12(1-\nu^2)}\left(1 - \frac{\theta h^2}{\beta}\frac{\partial^2}{\partial \alpha_1^2}\right)\frac{\partial^4 \psi_1}{\partial \alpha_1^4} + \left(1 - \frac{h^2}{\beta}\frac{\partial^2}{\partial \alpha_1^2}\right)\left[k_{22}^2(\alpha_2)\psi_1 + \frac{\rho_0}{E}\frac{\partial^2 \psi_1}{\partial t^2}\right] = 0. \tag{2.128}$$

It is of interest to note that the edge effect equation written in terms of the normal displacement w has the same form

$$\frac{h^2\eta_3}{12(1-\nu^2)}\left(1 - \frac{\theta h^2}{\beta}\frac{\partial^2}{\partial \alpha_1^2}\right)\frac{\partial^4 w}{\partial \alpha_1^4} + \left(1 - \frac{h^2}{\beta}\frac{\partial^2}{\partial \alpha_1^2}\right)\left[k_{22}^2(\alpha_2) w + \frac{\rho_0}{E}\frac{\partial^2 w}{\partial t^2}\right] = 0. \tag{2.129}$$

In Eqs. (2.128), (2.129), terms proportional to $h^2/(R^2\beta)$ account for shear. When $\beta \to \infty$ ($G \to \infty$), Eq. (2.129) degenerates into the classical equation of the dynamical edge effect for a thin isotropic single layer shell in the Kirchhoff-Love hypotheses based theory. The properties of integrals of this equation are described in detail in Gol'denveizer (1961); Gol'denveizer et al (1979).

Equation (2.122) is independent of Eqs. (2.128), (2.129) and has two the exponentially decaying partial solutions. Its general solution is

$$\psi_2 = C_1 \exp\left[-\frac{1}{h}\sqrt{\frac{2\beta}{1-\nu}}(\alpha_1 - \alpha_1^*)\right] + C_2 \exp\left[-\frac{1}{h}\sqrt{\frac{2\beta}{1-\nu}}(\alpha_1^{**} - \alpha_1)\right], \tag{2.130}$$

where C_i are arbitrary constants. Now consider Eq. (2.128) or (2.129). Let Z be any of unknown functions (w, ψ_1 or any other). In static problems (including buckling ones based on the static Euler criteria) the inertia term $\partial^2 Z/\partial t^2$ is absent. Then, if $k_{22} \neq 0$, then Eqs. (2.128), (2.129) degenerate into the governing equations for the simple edge effect in the static shell theory accounting for shear. At $k_{22} = 0$ and $\partial^2 Z/\partial t^2 \neq 0$, one obtains the dynamic equations for laminated plates.

The properties of partial solutions of Eq. (2.129) depends strongly on the order of the reduced shear modulus G with respect to the reduced Young's modulus E. The case when $G \sim E$ is not considered here, because in this case $\beta \sim 1$ and Eq. (2.129) has solutions with the index of variation $\iota_1 = 1$. Let $Z = \hat{Z}e^{\mathrm{i}\omega t}$ and ω is a natural frequency of free vibrations.

Case 1. Let $G \sim h_* E$. Then $\beta \sim h_*$ and $K_1 = \frac{h^2}{\beta R^2} \sim h_* \sim \mu^2$, where

$$\mu^4 = \frac{h^2 \eta_3}{12(1-\nu^2)R^2}. \tag{2.131}$$

Then Eq. (2.129) may be rewritten in the dimensionless form which is more convenient for the asymptotic analysis

$$-\mu^6 \kappa\theta \frac{\partial^6 X}{\partial x^6} + \mu^4 \frac{\partial^4 X}{\partial x^4} - \mu^2 \kappa \left[k_2(\varphi) - \Lambda\right] \frac{\partial^2 X}{\partial x^2} + \left[k_2(\varphi) - \Lambda\right] X = 0. \tag{2.132}$$

Here

$$\begin{aligned} &w = \hat{w}e^{\mathrm{i}\omega t}, \quad \hat{w} = RX(x), \quad \alpha_1 = Rx, \quad \alpha_2 = R\varphi, \\ &K_1 = \mu^2\kappa, \quad k_2(\varphi) = Rk_{22}[R(\varphi)] \sim 1, \quad \Lambda = \frac{R^2\rho_0\omega^2}{E}. \end{aligned} \tag{2.133}$$

As shown by Gol'denveizer et al (1979), in the theory of thin elastic isotropic shells based on the Kirchhoff-Love hypotheses, the frequency parameter Λ satisfies the following asymptotic estimates

$$\Lambda = O\left(h_*^{2-4\iota}\right) \quad \text{if} \quad 1/2 \leq \iota < 1 \tag{2.134}$$

and

$$\Lambda \sim h_*^{2-4\iota} \quad \text{for} \quad 0 \leq \iota < 1/2, \tag{2.135}$$

where $\iota = \max\{\iota_1, \iota_2\}$ is the general index of variation of the stress-strain state. The definition of the symbol O is given in Chapt. 6. We remind (Gol'denveizer et al, 1979) that estimate (2.134) corresponds to the quasi-transverse vibrations, and case (2.135) does to the Rayleigh type vibrations.

Equations of the technical theory of laminated shells, derived in subsection 2.1.11, are valid in particular for cases when $\iota = 1/2$ and $\iota = 1/4$. So, estimates (2.134), (2.135) may be applied for the analysis of Eq. (2.132). The type of the edge integrals and their properties depend on the sign of the expression $\delta = k_2 - \Lambda$ in Eq. (2.132). If $\iota = 1/4$, then $\delta(\varphi) > 0$ for any φ, and when $\iota = 1/2$, then the positive sign may be changed for the opposite one for all φ. The case when $\delta(\varphi)$ changes the sign under variation of φ is not considered here.

Omitting calculations, we will give the approximate (asymptotic) estimations for the partial solutions of (2.132). Regardless of the sign of δ, this equation has the following two integrals

$$X_1 = \mathrm{e}^{-\frac{1}{\mu}\sqrt{\frac{1}{\theta\kappa}}(x - x^*)}[1 + O(\mu)], \quad X_2 = \mathrm{e}^{-\frac{1}{\mu}\sqrt{\frac{1}{\theta\kappa}}(x^{**} - x)}[1 + O(\mu)] \tag{2.136}$$

where $x(\varphi)^* \le x \le x^{**}(\varphi)$, and $x^* = \alpha^*/R$, $x^{**} = \alpha^{**}/R$.

Now, we assume that the inequality

$$\delta = k_2 - \Lambda > 0 \tag{2.137}$$

holds for any φ. Here, there are three different cases:

1) Let $\kappa > 2/\delta$ for any φ. Then, with accuracy up to the values of order $O(\mu)$, Eq. (2.132) gives the following four additional integrals

$$\begin{aligned} X_3 &\approx \mathrm{e}^{-\frac{1}{\mu}\sqrt{\frac{\kappa\delta + \sqrt{\kappa^2\delta^2 - 4\delta}}{2}}(x - x^*)}, \\ X_4 &\approx \mathrm{e}^{-\frac{1}{\mu}\sqrt{\frac{\kappa\delta + \sqrt{\kappa^2\delta^2 - 4\delta}}{2}}(x^{**} - x)}, \\ X_5 &\approx \mathrm{e}^{-\frac{1}{\mu}\sqrt{\frac{\kappa\delta - \sqrt{\kappa^2\delta^2 - 4\delta}}{2}}(x - x^*)}, \\ X_6 &\approx \mathrm{e}^{-\frac{1}{\mu}\sqrt{\frac{\kappa\delta - \sqrt{\kappa^2\delta^2 - 4\delta}}{2}}(x^{**} - x)}. \end{aligned} \tag{2.138}$$

2) It is assumed that $\kappa < 2/\delta$ for any φ. Then

$$\begin{aligned} X_3 &\approx \mathrm{e}^{-\frac{\delta}{\mu}(r_1 + \mathrm{i}r_2)(x - x^*)}, \quad X_4 \approx \mathrm{e}^{-\frac{\delta}{\mu}(r_1 + \mathrm{i}r_2)(x^{**} - x)}, \\ X_5 &\approx \mathrm{e}^{-\frac{\delta}{\mu}(r_1 - \mathrm{i}r_2)(x - x^*)}, \quad X_4 \approx \mathrm{e}^{-\frac{\delta}{\mu}(r_1 - \mathrm{i}r_2)(x^{**} - x)}, \end{aligned} \tag{2.139}$$

where $\mathrm{i} = \sqrt{-1}$ is the imaginary unit, and

$$r_1 = \cos\left(\frac{1}{2}\arctan\frac{\sqrt{4\delta-\kappa^2\delta^2}}{\kappa\delta}\right), \quad r_2 = \sin\left(\frac{1}{2}\arctan\frac{\sqrt{4\delta-\kappa^2\delta^2}}{\kappa\delta}\right).$$

3) Let $\kappa = 2/\delta$, where $k_2 = 1$ (a circular cylindrical shell). Then, one has

$$X_3 \approx \mathrm{e}^{-\frac{1}{\mu}\delta^{1/4}(x-x^*)}, \quad X_4 \approx \mathrm{e}^{-\frac{1}{\mu}\delta^{1/4}(x^{**}-x)},$$
$$X_5 \approx x\,\mathrm{e}^{-\frac{1}{\mu}\delta^{1/4}(x-x^*)}, \quad X_6 \approx x\,\mathrm{e}^{-\frac{1}{\mu}\delta^{1/4}(x^{**}-x)}. \tag{2.140}$$

The variant when the expression $\kappa - 2/\delta$ changes the sign at some line $\varphi = \varphi_*$ for a non-circular shell is not considered here.

It is seen that for $\kappa > 2/\sqrt{\delta}$, all partial solutions of Eq. (2.132) are not oscillating functions but exponentially decaying far from the edges. If $\kappa < 2/\sqrt{\delta}$, then Eq. (2.132) has four the oscillating and decaying integrals (2.139) and two the exponentially decreasing solutions (2.136).

Now, let

$$\delta = k_2 - \Lambda < 0 \tag{2.141}$$

for any φ. Then, in addition to the partial solutions (2.136), Eq. (2.132) has only the two integrals

$$X_3 \approx \mathrm{e}^{-\frac{1}{\mu}\sqrt{\frac{\kappa\delta+\sqrt{\kappa^2\delta^2-4\delta}}{2}}(x-x^*)},$$
$$X_4 \approx \mathrm{e}^{-\frac{1}{\mu}\sqrt{\frac{\kappa\delta+\sqrt{\kappa^2\delta^2-4\delta}}{2}}(x^{**}-x)} \tag{2.142}$$

with the properties of the edges effect integrals, and the last two partial solutions are the oscillating functions which are not written down here. Thus, in case (2.141), the edge effect equation (2.132) has only four the exponentially decaying integrals. It should be noted that the decay rate of functions (2.136) is higher than that of the remaining integrals. Indeed, a parameter θ is small. If we assume that $\theta \sim h_*^{\sigma_\theta}$, where $\sigma_\theta > 0$, then the index of variation for integrals (2.136) will be equal to $\iota_1 = (1+\sigma_\theta)/2$. Then, for integrals (2.136) to be asymptotically correct and satisfy the accuracy of our model, it should be assumed the inequality $\sigma_\theta < 1$. Thus, if $G \sim h_* E$, then the index of variation of the both integrals (2.136) lies in the interval $1/2 < \iota < 1$, and the index of variation for the remaining four integrals equals $\iota = 1/2$ as in the Kirchhoff-Love model.

Case 2. Now, we consider the case when $G \sim h_*^{3/2} E$. This estimate holds if a shell is assembled, for instance, out of elastic layers and cores made of a magnitorheological elastomer (s. Sect. 2.3). Here, $K_1 \sim h_*^{1/2}$ and Eq. (2.129) is rewritten as follows

$$-\mu^5\kappa\theta\frac{\partial^6 X}{\partial x^6}+\mu^4\frac{\partial^4 X}{\partial x^4}-\mu\kappa\left[k_2(\varphi)-\Lambda\right]\frac{\partial^2 X}{\partial x^2}+\left[k_2(\varphi)-\Lambda\right]X=0, \quad (2.143)$$

where $K_1=\mu\kappa$, $\kappa\sim 1$, and the remaining magnitudes are introduced by (2.133). The asymptotic analysis of Eq. (2.143) gives two the exponentially decreasing functions

$$X_1=\mathrm{e}^{-\frac{1}{\mu^{1/2}}\sqrt{\frac{1}{\kappa}}(x-x^*)}[1+O(\mu)],$$
$$X_2=\mathrm{e}^{-\frac{1}{\mu^{1/2}}\sqrt{\frac{1}{\kappa}}(x^{**}-x)}[1+O(\mu)] \quad (2.144)$$

If $\delta>0$, then one obtains the additional four oscillating and decaying integrals,

$$X_3\approx\mathrm{e}^{-\frac{1}{\mu}\sqrt[4]{\frac{\delta}{4\theta}}(1+\mathrm{i})\,(x-x^*)},\quad X_4\approx\mathrm{e}^{-\frac{1}{\mu}\sqrt[4]{\frac{\delta}{4\theta}}(1+\mathrm{i})\,(x^{**}-x)},$$
$$X_5\approx\mathrm{e}^{-\frac{1}{\mu}\sqrt[4]{\frac{\delta}{4\theta}}(1-\mathrm{i})\,(x-x^*)},\quad X_6\approx\mathrm{e}^{-\frac{1}{\mu}\sqrt[4]{\frac{\delta}{4\theta}}(1-\mathrm{i})\,(x^{**}-x)}. \quad (2.145)$$

When $\delta<0$, Eq. (2.143) has only two the exponentially decreasing solutions,

$$X_3\approx\mathrm{e}^{-\frac{1}{\mu}\sqrt[4]{\frac{-\delta}{\theta}}\,(x-x^*)},\quad X_4\approx\mathrm{e}^{-\frac{1}{\mu}\sqrt[4]{\frac{-\delta}{\theta}}\,(x^{**}-x)}, \quad (2.146)$$

and the remaining two partial solutions are oscillating functions and not written down here. Taking into account the smallness of a parameter θ, one can conclude that the index of variation of integrals (2.145), (2.146) is larger than $1/2$. Assuming the estimate $\theta\sim h_*^{\sigma_\theta}$, we should to require the inequality $\sigma_\theta<2$.

So, in Case 2 (at $G\sim h_*^{3/2}E$), the properties of the edge effect integrals drastically differ from the ones of similar integrals in the classical Kirchhoff-Love model: two integrals (2.144) have the index $\iota=1/4$ and they may be carefully applied for the correction of the main stress state having the same index of variation and can not be considered as a correction for the state with more high index of variation; the remaining four integrals (2.145) (if $\delta>0$) or two ones (2.146) (at $\delta<0$) possess the index of variation $\iota=1/2+\sigma_\theta/4<1$ which is larger than this index in the classical theory. Integrals (2.145) or (2.146) may be used to correct the main stress state with the index of variation $\iota\leq 1/2$. The index of variation of the shear parameter ψ_2 (s. Eq. (2.130)) also depends on the order of the reduced shear parameter G. When $G\sim h_*E$, then $\iota_1=1/2$, and for $G\sim h_*^{3/2}E$, one has $\iota_1=1/4$.

2.1.15 Governing Equations for Laminated Plates and Beams

In this item we shall consider governing equations for laminated plates and beams. They are derived, as particular cases, form equations for cylindrical shells.

2.1.15.1 Laminated Plates

Let the curvature $k_{22} = 0$. Then Eqs. (2.77), (2.87) degenerate into the nonlinear differential equations for a laminated plate

$$D\left(1-\frac{\theta h^2}{\beta}\triangle\right)\triangle^2\chi - F_{,22}\left(1-\frac{h^2}{\beta}\triangle\right)\chi_{,11} + 2F_{,12}\left(1-\frac{h^2}{\beta}\triangle\right)\chi_{,12} - F_{,11}\left(1-\frac{h^2}{\beta}\triangle\right)\chi_{,22} = q_{\rm n} - \rho_0 h\frac{\partial^2}{\partial t^2}\left(1-\frac{h^2}{\beta}\triangle\right)\chi, \tag{2.147}$$

$$\triangle^2 F - Eh\left\{\left[\left(1-\frac{h^2}{\beta}\triangle\right)\chi_{,12}\right]^2 - \left(1-\frac{h^2}{\beta}\triangle\right)\chi_{,11}\left(1-\frac{h^2}{\beta}\triangle\right)\chi_{,22}\right\} = 0. \tag{2.148}$$

For $w \ll h_* R$, these equations may be linearized, they reducing to the two independent equations for the displacement and stress functions:

$$D\left(1-\frac{\theta h^2}{\beta}\triangle\right)\triangle^2\chi = q_{\rm n} - \rho_0 h\frac{\partial^2}{\partial t^2}\left(1-\frac{h^2}{\beta}\triangle\right)\chi, \tag{2.149}$$

$$\triangle^2 F = 0. \tag{2.150}$$

Let the plate rests on an elastic foundation with a modulus of subgrade reaction $c_{\rm f}$. Then Eq. (2.149) should be supplemented by the reaction force acting from the foundation:

$$D\left(1-\frac{\theta h^2}{\beta}\triangle\right)\triangle^2\chi + \left(c_{\rm f} + \rho_0 h\frac{\partial^2}{\partial t^2}\right)\left(1-\frac{h^2}{\beta}\triangle\right)\chi = q_{\rm n}. \tag{2.151}$$

The simplest model simulating the subgrade reaction is the Winkler foundation model. According to this model the spring constant $c_{\rm f}$ depends only on elastic properties of the foundation and is independent of the wave formation pattern of a plate. The detailed analysis of the response of an elastic foundation appears in Morozov and Tovstik (2010); Tovstik (2005). This analysis shows that the spring constant $c_{\rm f}$ depends on a number of waves on the surface of a thin-walled structure. Let the plate deflection be a periodic function of the coordinate α_1, α_2: $\chi = \chi_0 \sin k_1\alpha_1 \sin k_2\alpha_2$. Then, when assuming the rigid contact between the plate and foundation, one has

$$c_{\rm f} = \alpha_{\rm f} k, \quad \alpha_{\rm f} = \frac{2E_{\rm f}(1-\nu_{\rm f})}{(1+\nu_{\rm f})(3-4\nu_{\rm f})}, \quad k = \sqrt{k_1^2 + k_2^2}, \tag{2.152}$$

where E_{f} and ν_{f} are the Young's modulus and Poison's ratio for the foundation. Eq. (2.152) has been obtained for an infinite plate rested on an elastic half-space. Therefore, the range of applicability of Eq. (2.151) is restricted by the following conditions:

1. it is valid far from the plate edges;
2. a foundation has to be sufficiently deep;
3. forces of inertia of a foundation are not taking into account.

2.1.15.2 Laminated Beams

Equation (2.151) may be readily reduced to the governing equation for a beam. We shall consider a laminated beam with the rectangular cross section with sides $h \times b$, where b is the beam width, and h is the total thickness of the beam. Let q_{n} and all required functions be independent of α_2. To proceed to the beam model, one needs to assume that ν_k, all functions with index 2, and derivatives of these functions with respect to α_2 are equal to zero in all foregoing equations. Then, multiplying Eq. (2.151) by b, one obtains the following equation

$$EI\eta_3\left(1-\frac{\theta h^2}{\beta}\frac{\partial^2}{\partial\alpha_1^2}\right)\frac{\partial^4\chi}{\partial\alpha_1^4}+\left(c_{\mathrm{f}}'+\rho_l\frac{\partial^2}{\partial t^2}\right)\left(1-\frac{h^2}{\beta}\frac{\partial^2}{\partial\alpha_1^2}\right)\chi=q_{\mathrm{l}}(\alpha_1,t), \tag{2.153}$$

where

$$I=\frac{h^3b}{12},\quad \rho_{\mathrm{l}}=\rho_0bh,\quad q_{\mathrm{l}}=q_{\mathrm{n}}b,\quad c_{\mathrm{f}}'=c_{\mathrm{f}}b.$$

Here, I is the area moment 2nd order of the beam cross section, $\rho_{\mathrm{l}}, q_{\mathrm{l}}$ are the linear mass and load, respectively. Note also that θ, β, η_3 are calculated at $\nu_k = \nu = 0$.

Equation (2.153) should be supplemented by the one-dimensional equation (2.85) for ϕ. However, as will be shown below, the trivial solution $\phi = 0$ is the unique solution satisfying the appropriate boundary conditions for a beam. When $G \to \infty$ that means $\beta^{-1} \to 0$, then Eq. (2.153) degenerate into the classical equation which does not take shears into account.

2.2 Governing Equations of Shell Buckling

In this section we consider the principle equations which will be used in Chapt. 3 for the buckling analysis of thin laminated elastic cylindrical shells. The governing equations are derived from the geometrically non-linear equations obtained in the previous chapter. The physically non-linear formulation of the buckling problem, assuming the non-linear coupling of stresses on strains, is not considered below. The derived equations describe the bifurcation (branching) of both the moment and in-plane equilibrium stress-strain states. They are valid for cases when the shell thickness is small and buckling occurs with minor sizes of deflections.

2.2.1 Bending Stress State

In common case, buckling equations for a thin laminated cylindrical shell may be derived by considering variations of the full system of the nonlinear differential Eqs. (2.61)-(2.63), in which the inertia terms should be omitted. In this section, we consider the case when buckling occurs with minor sizes of dents at least at one of the directions at the shell surface. Then the simplified nonlinear equations (2.77), (2.85) and (2.87) of the technical theory of laminated shells written in terms of the functions F, χ, ϕ may be used as the initial ones.

It is assumed here and in what follows that the shell is under action of only conservative surface and/or edge loads. The load is called conservative, if the work done by it depends only on the end states of the shell and does not depend on the way of deformation. Problems on dynamic stability of the shell experiencing dynamic and non-conservative loads are not considered here. Solutions of similar problems may be found, for instance, in Lavrent'ev and Ishlinsky (1949); Srubschik (1985, 1988); Vol'mir (1972, 1976); Bolotin (1956); Fung and Sechler (1974). It should be noted that only the dynamic criterion gives accurate results for shells subjected to both dynamic and static non-conservative loads (Ziegler, 1968; Bolotin, 1956).

Let

$$F^\circ, \quad \chi^\circ, \quad \phi^\circ \tag{2.154}$$

be functions describing the initial (pre-buckling) stress state of a laminated cylindrical shell. Then, as follows from subsection 2.1.11, all the kinematic characteristics (normal deflection w°, generalized displacements $\hat{u}_i^\circ$, and angles of rotation ψ_i°) as well as the stress characteristics (in-plane stresses T_{ij}° and generalized moments $\hat{M}_{ij}^\circ, \hat{L}_{ij}^\circ$) are identically determined through the functions $F^\circ, \chi^\circ, \phi^\circ$. The functions $F^\circ, \chi^\circ, \phi^\circ$ or $w^\circ, \hat{u}_i^\circ, \psi_i^\circ, T_{ij}^\circ, \hat{M}_{ij}^\circ, \hat{L}_{ij}^\circ$ may be found from the linearized Eqs. (2.61)-(2.63), or (2.77), (2.85) and (2.87).

Following Euler, we consider the adjacent stress state which is infinitesimally close to the pre-buckling one and characterized by unknown functions

$$F^\circ + F, \quad \chi^\circ + \chi, \quad \phi^\circ + \phi. \tag{2.155}$$

Let us substitute functions (2.155) into the non-linear Eqs. (2.77), (2.85) and (2.87). Then, taking into account the fact that functions (2.155) satisfy the nonhomogeneous Eqs. (2.77), (2.85) and (2.87) with appropriate boundary conditions (which are not uniform in the common case) and performing linearization in a neighbourhood of the stress state characterized by (2.154), one obtains the following homogeneous buckling equations

$$
\begin{aligned}
&D\left(1-\frac{\theta h^2}{\beta}\Delta\right)\Delta^2\chi-\frac{\partial^2 w^\circ}{\partial\alpha_1^2}\frac{\partial^2 F}{\partial\alpha_2^2}+2\frac{\partial^2 w^\circ}{\partial\alpha_1\partial\alpha_2}\frac{\partial^2 F}{\partial\alpha_1\alpha_2}\\
&+\left(\frac{1}{R_2}-\frac{\partial^2 w^\circ}{\partial\alpha_2^2}\right)\frac{\partial^2 F}{\partial\alpha_1^2}-T_{11}^\circ\frac{\partial^2 w}{\partial\alpha_1^2}-2T_{12}^\circ\frac{\partial^2 w}{\partial\alpha_1\partial\alpha_2}-T_{22}^\circ\frac{\partial^2 w}{\partial\alpha_2^2}=0,\\
&\Delta^2 F=Eh\left(\frac{1}{R_2}\frac{\partial^2 w}{\partial\alpha_1^2}+2\frac{\partial^2 w^\circ}{\partial\alpha_1\partial\alpha_2}\frac{\partial^2 w}{\partial\alpha_1\partial\alpha_2}-\frac{\partial^2 w^\circ}{\partial\alpha_2^2}\frac{\partial^2 w}{\partial\alpha_1^2}-\frac{\partial^2 w^\circ}{\partial\alpha_1^2}\frac{\partial^2 w}{\partial\alpha_2^2}\right),\\
&w=\left(1-\frac{h^2}{\beta}\Delta\right)\chi,\qquad \frac{1-\nu}{2}\frac{h^2}{\beta}\Delta\phi=\phi,
\end{aligned}
\tag{2.156}
$$

where

$$
w^\circ=\left(1-\frac{h^2}{\beta}\Delta\right)\chi^\circ. \tag{2.157}
$$

When deriving Eq. (2.156), we used the introduced above Eq. (2.74)

$$
T_{ij}^\circ=\delta_{ij}\Delta F^\circ-\frac{\partial^2 F^\circ}{\partial\alpha_i\partial\alpha_j},\quad i,j=1,2. \tag{2.158}
$$

Equations (2.156) with appropriate homogeneous boundary conditions describe buckling of the moment stress state. If components of the external load (for instance, the external pressure q_{n} or the axial force T_{11}^*) are weakly varying functions of α_1, α_2, then the initial moment stress state may be found as a sum of the membrane stress state and the edge effect (Tovstik and Smirnov, 2001). The in-plane (momentless) stress state are determined by the stress-resultants T_{ij}° which are found from equations of the membrane shell theory, s. Eqs. (2.67), in which the inertia terms are omitted. The edge effect described by the displacement w° may be determined from the edge effect equation (2.129)

$$
D\left(1-\frac{\theta h^2}{\beta}\frac{\mathrm{d}^2}{\mathrm{d}\alpha_1^2}\right)\frac{\mathrm{d}^4 w}{\mathrm{d}\alpha_1^4}+\frac{Eh}{R_2^2}\left(1-\frac{h^2}{\beta}\frac{\mathrm{d}^2}{\mathrm{d}\alpha_1^2}\right)w=0. \tag{2.159}
$$

2.2.2 In-plane Stress State

Let the external load be such that the initial (pre-buckling) displacements u_i°, w° and the in-plane stress resultants T_{ij}° characterizing this state, are weakly varying functions of the curvilinear coordinates α_1, α_2. Then, the neutral surface before and after deformation may be identified (Tovstik and Smirnov, 2001). In other words, we may assume that being in the pre-buckling state the shell is stressed but not deformed (Alfutov, 2000). For this state called the in-plane stress state, it is assumed that $w^\circ = 0$. Then the buckling equations (2.156) are simplified

$$D\left(1-\frac{\theta h^2}{\beta}\Delta\right)\Delta^2\chi+\frac{1}{R_2}\frac{\partial^2 F}{\partial\alpha_1^2}-\Delta_T w=0,$$
$$\Delta^2 F=\frac{Eh}{R_2}\frac{\partial^2 w}{\partial\alpha_1^2},\quad w=\left(1-\frac{h^2}{\beta}\Delta\right)\chi, \tag{2.160}$$
$$\frac{1-\nu}{2}\frac{h^2}{\beta}\Delta\phi=\phi,$$

where

$$\Delta_T w=T^\circ_{11}\frac{\partial^2 w}{\partial\alpha_1^2}+2T^\circ_{12}\frac{\partial^2 w}{\partial\alpha_1\partial\alpha_2}+T^\circ_{22}\frac{\partial^2 w}{\partial\alpha_2^2}, \tag{2.161}$$

and the in-plane stress-resultants T°_{ij} are found from the stationary counterparts of Eqs. (2.67) of the moment-less shell theory.

The differential equations (2.160) with an appropriate variant of boundary conditions (2.109)-(2.117) describe buckling of the in-plane stress state of a thin laminated shell. If the initial state is presented by the full system of in-plane stress resultants T°_{ij} (for instant, at combined loading), it is convenient to assume that the in-plane forces vary proportionally to a loading parameter λ

$$T^\circ_{ij}=\lambda t^\circ_{ij}. \tag{2.162}$$

Then the buckling problem is reduced to an eigenvalue problem which is to find the least positive $\lambda=\lambda^*$ for which this problem has a nontrivial solution. Found in this way the parameter λ^* is called buckling or critical loading parameter.

Equations (2.160) will be used in the next chapter for studying a number problems on the local buckling of thin sandwich and multi-layered cylindrical shells under different variant of loading. Note that at $\beta^{-1}\to 0$ (implying $G\to\infty$) Eqs. (2.160) degenerate into the well-known buckling equations of the technical theory of thin isotropic single layer shells which are based on the original Kirchhoff-Love hypothesis and were widely utilized by many researchers for investigation of an enormous number of problems (Donnell, 1976; Grigolyuk and Kabanov, 1978; Tovstik and Smirnov, 2001).

2.3 Laminated Cylindrical Shells with Viscoelastic Smart Layers

This section deals with laminated shells assembled from elastic and viscoelastic damping layers. In case of the harmonic response, elastic and viscous properties of damping layers are represented by the complex forms for Young's and shear moduli. It is discussed that smart materials, such as magnetorheological elastomers and electrorheological composites, may be used as damping elements of sandwich or multi-layered thin-walled structures. The mechanical and rheological properties of some smart viscoelastic magneto- and electrorheological materials affected by applied magnetic or electric field are given. The applicability of the equivalent single layer model for laminated shells with soft viscoelastic layers or cores is also discussed.

2.3.1 Viscoelastic Materials in Thin-walled Laminated Structures

Viscoelastic damping materials (VDMs) are used widely in thin-walled laminated structures. The traditional roles of their application usually are:

a) free layer damping (FLD);
b) constrained layer damping (CLD) (Zhou et al, 2015);
c) core damping (CD).

In the first case a), VDM is attached to the surface of an elastic layer, its outer surface being free. Earliest researches on application of VDMs in the capacity of FLD began in the early 1950s, by Oberst and Frankenfeld (1952) and Mead and Ae (1960).

In case b), VDM attached to the basic elastic lamina is in turn constrained by a backing very thin elastic layer or foil. A common example of CLD is the damping tape currently used in aircrafts. Kervin Jr. (1959); Ross et al (1959); Ungar and Kerwin Jr. (1962) may be the first studies where a quantitative analysis on the damping effectiveness of CLD was performed. After these research works, there were many other papers (e.g, s. DiTaranto, 1965; Mead and Markus, 1970; Yan and Dowell, 1972; Kumar and Singh, 2010; Wang and Chen, 2004; Raamesh and Ganesan, 1994) on vibrations of thin plates, beams, curved panels, cylindrical shells, and sandwiched structures tackled by CLD. The application of constrained viscoelastic treatments for improving damping capabilities became a very popular method in the case of thin-walled structures made of materials (e.g., steel, aluminium) which possess a little material damping. As a rule, a backing layer constraining VDM does not influence essentially the total stiffness of a thin-walled structure.

In the third variant c), VDM is embedded between two elastic layers, so that an assembled structure looks like a sandwich. In this case, both elastic layers are, as a rule, considerably stiffer than a soft VDM and serve as the bearing elements which define the total stiffness of a structure, whereas the embedded viscoelastic core ensures the damping mechanism. In the same way, multi-layered beams, plates or shells with alternating elastic and viscoelastic layers may be assembled. Pan (1969); Mead and Markus (1969), and DiTaranto (1965) must be the first who considered problems on damped vibrations of three-layered or multi-layered beams and shells with viscoelastic cores. By now, there are many papers which deal with different aspects of the influence of VDM as of damping core on suppression of vibrations of both sandwich and laminated thin-walled structures (s., among many others, Khatri, 1996; Zhou and Rao, 1996; Yu and Huang, 2001; Matter et al, 2011; Schwaar et al, 2011) and the survey article of Qatu et al (2010).

The damping capability of VDMs in a laminated structure depends not only on their viscous properties, but on densities of materials composing a structure, a number of layers (Saravanan et al, 2000) and correlations between thicknesses of elastic and viscolelastic laminas as well (Yan and Dowell, 1972; Hu and Huang, 2000; Jin et al, 2015).

2.3.2 Complex Moduli of Viscoelastic Materials

There are different theories on viscoelasticity and various models describing the dynamic response of the VDM (e.g., the simplest well known models of Maxwell and Kelvin-Voigt, their generalization to the Kelvin chain model (Parke, 1966) and Biot's one (Biot, 1958), numerous non-linear models listed in Bert (1947), the hereditary theory of material damping (Boltzmann, 1878; Gross, 1947; Volterra, 1950) and their subsequent generalizations, very popular fractional models as specific cases of the so-called hereditary continuous media (Koeller, 1984; Cosson and Michon, 1996, and many others).

The application of one or another model of a viscoelastic material depends on both its type and the character of the dynamic response of a structure. For instance, if a viscoelastic body or structure is subjected to the long-term exposure of external forces, or the force load is suddenly withdrawn and the non-stationary strain-stress state is characterized by the relaxation of stresses, then the hereditary theory of viscoelastic materials is usually applied. The fractional models are frequently used to study the dynamic response of elastomers (Cosson and Michon, 1996).

In the case of the harmonic (sinusoidal) response of polymers and elastomers, frequently utilized models are ones which are based on the assumption of the complex form for Young's and shear moduli (Kervin Jr., 1959; Ross et al, 1959)

$$E_{\mathrm{v}} = E'_{\mathrm{v}}(1 + \mathrm{i}\eta_1), \quad G_{\mathrm{v}} = G'_{\mathrm{v}}(1 + \mathrm{i}\eta_2), \tag{2.163}$$

where $E'_{\mathrm{v}}, G'_{\mathrm{v}}$ are storage moduli, and η_1, η_2 are loss factors. A storage modulus is a measure of VDM's elasticity and the loss factor determines how much energy will be dissipated in motion.

It is of interest to note that the first representation of stiffness in the complex form was given by Soroka (1949). According to Bert (1947), utilizing observations of Kimball and Lovell (1927) for many engineering VDMs, Soroka has proposed to replace the stiffness k in the undamped elastic system by the Kimball-Lovell *complex stiffness*

$$k = k' + \mathrm{i}k''. \tag{2.164}$$

Later, the viscoelastic models assuming the complex representation of the structural stiffness were used extensively in aircraft structural dynamic and flutter analyses (e.g., s. Scanlan and Rosenbaum, 1951).

In general case, for the VDM model represented by (2.163), the moduli $E_{\mathrm{v}}, G_{\mathrm{v}}$ are considered as independent magnitudes. If the VDM is assumed to be isotropic, then $E_{\mathrm{v}}, G_{\mathrm{v}}$ are coupled

$$G_{\mathrm{v}} = \frac{E_{\mathrm{v}}}{2(1+\nu)}, \tag{2.165}$$

where ν is Poison's ratio of the VDM. As a rule, ν is taken as a real parameter for a viscoelastic material.

Regardless of the role of the VDM (FLD, CLD or CD) in a thin-walled structure, the shear phenomenon is the original source with which the VDM dissipates energy and damps vibrations. An analysis of the effect of this shear damping mechanism was first given by Kervin Jr. (1959) when studying vibrations of a constrained viscoelastic plate. Recently, Jin et al (2015) confirmed that the high damping capacity of the viscoelastic layer is mainly due to the shear deformations of the VDM. Furthermore, it has been shown that there exists an optimal shear modulus of the viscoelastic core which results in the best damping performance for a sandwich cylindrical shell.

Thus, the complex shear modulus $G_\mathrm{v} = G'_\mathrm{v} + \mathrm{i}G''_\mathrm{v}$ turns out to be basic in the damping mechanism, and its real and imaginary parts $G'_\mathrm{v}, G''_\mathrm{v}$ may be influenced by many factors. So, in accordance with Kerwin-Douglas-Yang model (Kervin Jr., 1959; Douglas and Yang, 1978), the parameters $G'_\mathrm{v}, G''_\mathrm{v}$ depend on the frequency ω and temperature T. Later, performing the finite-element simulation and companion experiment on vibrations of a damped sandwich plates with the viscoelastic core made of a polymer material (which belongs to class A of thermorheologically simple materials), Lu et al (1979) justified this model. The empirical equations for $G'_\mathrm{v}(\omega, T)$ and $G''_\mathrm{v}(\omega, T)$ were obtained by Drake in 1990 for seven different VDMs (s. Rao and He, 1992; Zhou and Rao, 1996).

Due to the long-range molecular order associated with their giant molecules, polymers and elastomers exhibit rheological behavior intermediate between that of a crystalline solid and a simple liquid (Bert, 1947). Important physical properties of these VDMs are the marked dependence of both stiffness and damping on frequency and temperature. However, traditional viscoelastic material are not affected by the action of other physical fields (such as electrical and magnetic ones). Because of the predetermined and limited range of variation of the complex shear modulus G_v, they are generally used for passive damping of vibrations.

2.3.3 Smart Electro- and Magnetorheological Materials [2]

Smart materials are designed materials having properties that can be significantly changed in a controlled manner by external stimulation of mechanical, electrical, magnetic, etc. fields. They have a lot of applications, for example as sensors or actuators. Thee modelling of their constitutive behavior is more complicated since mechanical responses with other physical fields should be considered. Finally, one gets a material for which a non-mechanical stimulus, for example changing of electrical or magnetic fields, can be transformed into changes of strains and stresses. Examples of similar materials are piezoelectric and magnetostrictive materials, shape memory alloys, electrorheological composites, magnetorheological fluids and elastomers.

[2] This subsection is written in cooperation with E.V. Korobko (A.V. Lykov Heat and Mass Transfer Institute of National Academy of Sciences of Belarus, Minsk, Belarus, e-mail: evkorobko@gmail.com).

The integration of viscoelastic smart materials (VSM) with traditional elastic ones or passive VDMs is a key idea in the modelling of smart structures and, particularly, smart thin-walled laminated structures. Indeed, a smart thin laminated shell (STLS) is able to develop stiffness and damping characteristics which can change in dependence of changes of the acting physical fields. Such an behavior is not related to a shell structure made of a traditional material. From all variety of VSMs we will study here magnetorheological fluids and elastomers and electrorheological composites. They will be considered as semi-active layers or cores in laminated beams, plates, panels and shells with viscoelastic properties.

Composite magnetorheological (MR) materials consist of magnetic micro - particles inserted into a diamagnetic or paramagnetic fluid, or into an elastic or viscoelastic medium (matrix). The magnetic interaction between these particles depend on many factors: magnetization direction of particles and their space distribution, the orientation of external magnetic field and the strain field in a composite material. Depending on the type of medium where magnetic particles are placed to, one differentiates magnetorheological elastomers (MRE), gels (MRG) and fluids (MRF).

MREs are magnetizable particles molded in non-magnetic elastomeric or rubber-like materials (Farshad and Benine, 2004; Li et al, 2009, 2010) including natural deformed polymer matrices (Farshad and Benine, 2004), natural rubbers (Yang et al, 2013) and synthetic ones (Sun et al, 2008; Bica et al, 2014; Wang et al, 2006; Sun et al, 2008), and MRFs are liquid dispersions of magnetic particles (Wiess et al, 1994; Zhurauski et al, 2008).

Composite electrorheological (ER) material, more often electrorheological fluid (ERF), is suspension of dielectric particles of different concentration in a viscous medium (Hao et al, 1998; Zhurauski et al, 2008). These materials can change their rheological properties under the action of electrical fields. Some ERFs with high concentration of dielectric particles under the action of electrical field show viscoelastic properties very close to properties of elastomer. Similar high-density smart liquid is often called electrorheological composite (ERC).

It should be noted that MR and ER fluids have some lacks. The first problem existing in MR/ER fluids is the particle sedimentation. Secondly, they do not keep their geometrical shape at a low electric or magnetic field level that leads to some technological problems at designing and running the solid-fluid structures. It is solid smart materials such as MREs that are mostly applicable in the vibration control of STLS (Ginder et al, 2001).

Viscoelastic properties of MR/ER materials strongly depend on both composition and ratio of all components. The optimum weight/density ratio of magnetic or dielectric particles, carrier viscous liquid and/or polymer matrix substantially determines shear modulus, viscosity and response time of VSMs. As far as MREs, their properties are also influenced by the technology of production. If a MRE is produced in the absence of a magnetic field, it possesses by isotropic properties (Venkateswara et al, 2010; Zajac et al, 2010). On the contrary, when the polymerization reaction is carried out in an external homogeneous magnetic field, then a MRE becomes highly polarized (Korobko et al, 2009) medium having anisotropic properties (Stepanov et al, 2007; Kallio et al, 2007; Bica et al, 2015). Furthermore, experimental works (Boczkowska et al, 2012) demonstrate that the maximum increase in the storage modulus G'_{v} of the polarized MRE placed in the homogeneous magnetic field strongly depends on the particles arrangement within the matrix with respect to the force lines of a magnetic field.

In the next two items, we will consider MRE and ERC elaborated in the Laboratory of Rheophysics and Macrokinetics (LRM) of A.V. Luikov Heat and Mass Transfer Institute (LHMTI) of the National Academy of Sciences of Belarus. For comparison, the elastic and rheological properties of other available smart composites will be considered as well.

2.3.3.1 Magnetorheological Elastomers

Let us consider here the anisotropic MRE consisting of deformed polymer matrix and magnetic particles embedded in this matrix (Korobko et al, 2012). The procedure of manufacturing this MRE was the following. A natural inorganic polymer (bentonite clay, size of laminar particles is 1 - 10 μm) in the synthetic oil *Mobil SAE* was used as a matrix for the MRE, and particles of carbonyl iron (particle size is about 20 μm) as a filler. The matrix for the MRE was prepared by thorough rubbing the polymer in surfactant-added oil. Then carbonyl iron particles were introduced (about 22 vol. %) into the prepared matrix. Densities of components and their volume concentrations for this MRE (called in what follows as MRE-1) are presented in Table 2.1.

The real and imaginary parts, G'_{v} and G''_{v}, of the complex shear modulus G_{v} for this MRE have been obtained by the method of rotational viscometry. The rheometer *Physica MCR 301* (Anton Paar) with the "plate-plate" measuring nest in the range of the magnetic field induction up to 1 Tesla (T) has been used for the experimental measurements. The viscoelastic properties were defined at different values of the magnetic induction B and for the amplitude of deformations varying from 0.01 to 2 %. The frequency of deformations was taken to be equal to $0.1,\ 10,\ 100$ Hz.

Figures 2.5 and 2.6 show the effect of the strain amplitude and the magnetic induction B on the storage and loss moduli G'_{v} and G''_{v} for the frequency $\omega = 10$ Hz. It is seen that the MRE-1 placed in a magnetic field keeps elastic properties only at small shear strains in the pre-yield regime; when the amplitude of shear deformations increases, the MRE structure reaches the yield point and begins to fail displaying the viscous flow features. For the MRE under consideration, the pre-yield regime

Table 2.1 Volume concentrations of the MRE-1 components and their densities.

MRE comonents	Density, g/sm^3	Weight, g	Volume concentration, %
Particles of carbonyl iron	7.50	54.8	22
Bentonite clay	1.65	21.5	39
Oil *Mobil SAE*	0.85	10.0	35
Surfactant oil	0.94	1.0	3
Total	2.63	87.3	100

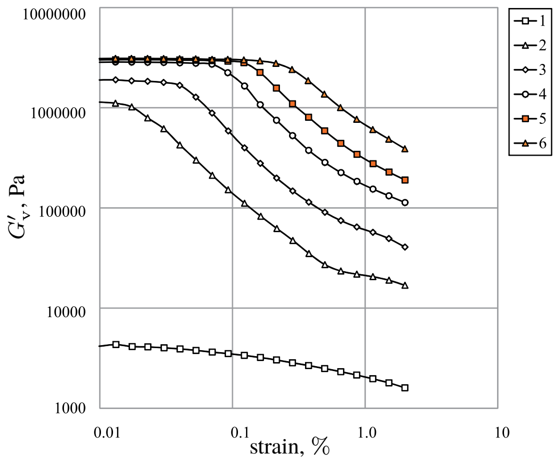

Fig. 2.5 Storage modulus G'_v of the MRE-1 vs. strain at the frequency $\omega = 10$ Hz for different values of the magnetic induction B:
1 - $B = 0$ mT,
2 - $B = 50$ mT,
3 - $B = 100$ mT,
4 - $B = 200$ mT,
5 - $B = 300$ mT,
6 - $B = 500$ mT.

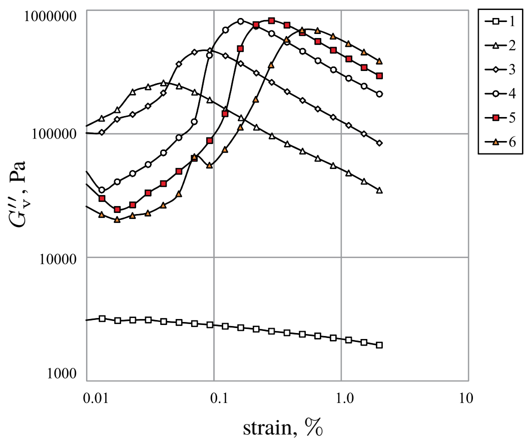

Fig. 2.6 Loss modulus G''_v of the MRE-1 vs. strain at the frequency $\omega = 10$ Hz for different values of the magnetic induction B:
1 - $B = 0$ mT,
2 - $B = 50$ mT,
3 - $B = 100$ mT,
4 - $B = 200$ mT,
5 - $B = 300$ mT,
6 - $B = 500$ mT.

strongly depends on the level of an applied magnetic field. In the absence of a magnetic field or for small values of B, the MRE pre-yield behavior is linearly viscoelastic only at very small shear deformations, but for $B = 300$ mT the pre-yield shear behavior is linearly viscoelastic for shear strains not exceeding $0.15\ \%$.

In Figs. 2.7 and 2.8, the dependence of the storage and loss moduli on the magnetic field induction are given for different frequencies of small shear deformations. As seen, under high frequency harmonic deformations of the MRE-1, the functions $G'_v(B), G''_v(B)$ display almost the same behavior. Thus, the storage and loss moduli of the MRE may be considered invariant with respect to the frequency of shear vibrations if this frequency exceeds about 10 Hz. These *invariants* (determined as average values in the frequency range from 10 to 100 Hz) versus the magnetic induction B are shown in Fig. 2.9 (Korobko et al, 2012). For the MRE-1, the maximum values of the storage and loss moduli, $\max G'_v \approx 3089$ kPa, $\max G''_v \approx 830$ kPa, are reached at $B \approx 500$ mT and $B \approx 250$ mT, respectively. The data presented in

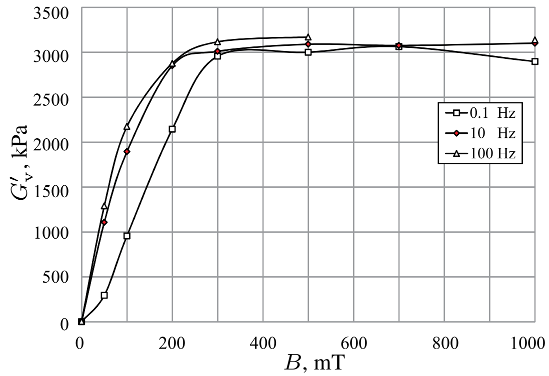

Fig. 2.7 Storage modulus G'_{v} of the MRE-1 vs. the magnetic induction B for different frequencies $\omega = 0.1; 10; 100$ Hz of excitation.

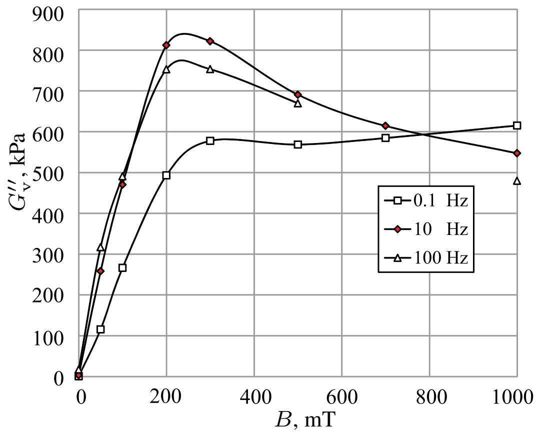

Fig. 2.8 Loss modulus G''_{v} of the MRE-1 vs. the magnetic induction B for different frequencies $\omega = 0.1; 10; 100$ Hz of excitation.

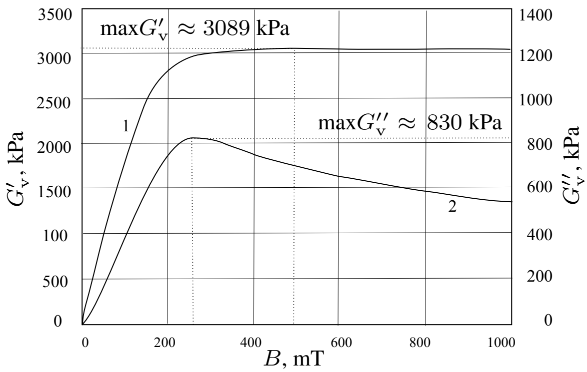

Fig. 2.9 Storage and loss moduli G'_{v} - line 1, G''_{v} - line 2 vs. the magnetic induction B for the MRE-1 (after Korobko et al, 2012).

Fig. 2.9 will be repeatedly used below for the analysis of damped vibrations of the MRE-based laminated beams, plates and shells. The major characteristic for a MRE is the loss factor which is determined by the ratio between the loss modulus G''_{v} and the storage modulus G'_{v} as

$$\eta_{\mathrm{v}} = \tan \delta_{\mathrm{v}} = \frac{G''_{\mathrm{v}}}{G'_{\mathrm{v}}}. \tag{2.166}$$

Figure 2.10 shows the effect of the applied magnetic field on the loss factor for the MRE-1 at different frequencies of shear deformations. One can see that at low-frequency oscillations of the sample, the loss factor η_{v} is the monotonically decreasing function of the magnetic induction B, but at frequencies exceeding 10 Hz there is a local maximum corresponding to the yield point of the MRE-1.

The analysis of actual researches reveals a large variety of MREs elaborated on the base of different polymeric materials. For comparison, we give here several examples of different MREs. The viscoelastic properties of the MRE-2 obtained by mixing the silicone oil and the RTV141A polymer with subsequent loading with 30% of ferromagnetic particles (Aguib et al, 2014) are presented in Table 2.2. According to Aguib et al (2014), the density of the MRE-2 equals 1.1 g/sm^3, Poisson's ratio is 0.44, and the Young' modulus is assumed to be the real constant magnitude, 1.7 MPa, independent of a magnetic field. So, the MRE-2 is treated as the transversally isotropic material.

Table 2.3 shows the compositions of different natural rubber based MREs elaborated by Chen et al (2008). For any of these elastomers, the matrix consists of the same components: 48.5% of natural rubber, 50% of plasticizers, and 1.5% of other additions. Properties of these MREs are presented in Tables 2.4-2.6.

When comparing properties of the MREs considered above, one can conclude that the MRE-1 possess the largest loss factor, and the MRE-5 with the highest content

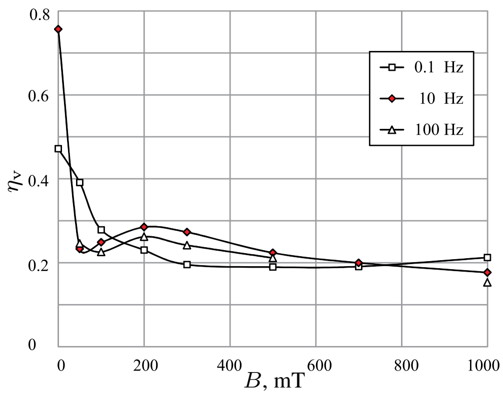

Fig. 2.10 Loss factor η_{v} for MRE-1 vs. the magnetic induction B at different frequencies of shear deformations.

Table 2.2 Storage and loss moduli G'_{v}, G''_{v} and loss factor η_{v} vs. the magnetic induction B for the MRE-2 (Aguib et al, 2014).

Magnetic induction B, mT	Storage modulus G'_{v}, kPa	Loss modulus G''_{v}, kPa	Loss factor η_{v}
0	1600	330	0.206
200	1760	500	0.284
350	1930	540	0.280
500	2070	350	0.170

Table 2.3 Composition of natural rubber based MREs elaborated by Chen et al (2008).

Sample	Magnetic particles, %	Carbon black, %	Matrix, %	Density, g/sm^3
MRE-3	33	0	67	1.895
MRE-4	33	4	63	1.872
MRE-5	33	7	60	1.855

Table 2.4 Storage and loss moduli G'_{v}, G''_{v} and loss factor η_{v} vs. the magnetic induction B for the MRE-3 (Chen et al, 2007) containing 33% of iron particles and 0% of carbon black.

Magnetic induction B, MT	Storage modulus G'_{v}, kPa	Loss modulus G''_{v}, kPa	Loss factor η_{v}
0	1000	220	0.22
200	1600	416	0.26
400	2100	504	0.24
600	2200	550	0.25
800	2300	1150	0.25

Table 2.5 Storage and loss moduli G'_{v}, G''_{v} and loss factor η_{v} vs. the magnetic induction B for the MRE-4 (Chen et al, 2007) containing 33% of iron particles and 4% of carbon black.

Magnetic induction B, mT	Storage modulus G'_{v}, kPa	Loss modulus G''_{v}, kPa	Loss factor η_{v}
0	2000	360	0.18
200	2200	440	0.20
400	2400	480	0.20
600	2500	500	0.20
800	2600	494	0.19

Table 2.6 Storage and loss moduli G'_{v}, G''_{v} and loss factor η_{v} vs. the magnetic induction B for the MRE-5 (Chen et al, 2008) containing 33% of iron particles and 7% of carbon black.

Magnetic induction B, mT	Storage modulus G'_{v}, kPa	Loss modulus G''_{v}, kPa	Loss factor η_{v}
0	4050	567	0.14
200	4250	723	0.17
400	6000	960	0.16
600	7900	1185	0.15
800	8000	1120	0.14

of carbon black has very large shear moduli. It is also interesting to note that adding carbon black results in the weak dependence of the loss factor on the magnetic field induction.

As mentioned above, viscoelastic properties of any MRE are very influenced by wether it is isotropic or anisotropic. Figure 2.11 illustrates the effect of a magnetic field on the storage modulus for the isotropic and anisotropic MREs with the matrix prepared from formoplast, which is a kind of silicon rubber (Demchuk and Kuzmin, 2002). The powder of iron with particles of the size about 23 μm was used as a filler for this MRE (called here as the MRE-6). It is seen that the orientation of magnetic

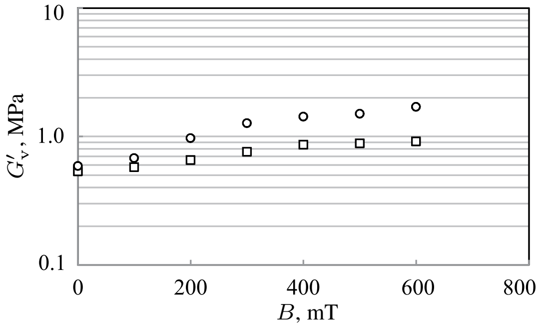

Fig. 2.11 Storage modulus G'_v (MPa) vs. the magnetic induction B (mT) for the isotropic and anisotropic MRE-6 (Demchuk and Kuzmin, 2002): □ - isotropic sample; ○ - anisotropic sample.

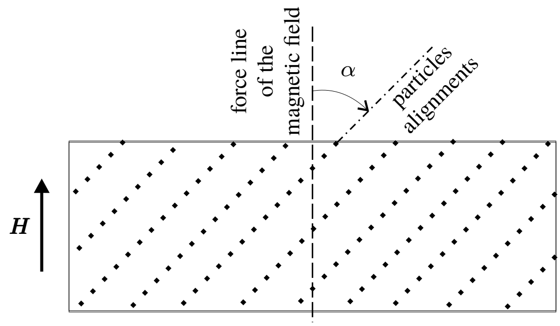

Fig. 2.12 Schematic representation of the particles alignment in the anisotropic MRE sample with reference to the force lines of the magnetic field.

particles influences the storage modulus: if a magnetic field is absent, this effect is weak, however in the magnetic field of a relatively high induction, the shear modulus of the anisotropic MRE-6 is about two times as much than for the isotropic sample.

The same effects were detected by other authors for the MREs made of natural rubber (Aguib et al, 2014) and polyurethane (Boczkowska et al, 2012). Furthermore, as follows from Boczkowska et al (2012); Kumar and Lee (2017), viscoelastic properties of a polarized MRE turn out to be very sensitive to the angle between the force lines of a magnetic field and the direction, in which the magnetic particles are aligned. In particular, samples of MREs with particles aligned perpendicular to the magnetic field (s. Fig. 2.12) and with isotropic distribution have exhibited relatively small rise in the storage modulus G'_v. But higher increase has been observed for the sample with parallel alignment ($\alpha = 0°$) and the highest for that with particle chains deflected at $\alpha = 45°$ and $\alpha = 30°$. So, at the frequency $\omega \approx 90$ Hz, the modulus G'_v for the sample with $\alpha = 30°$ was about 3.5 times as much than that for the sample with $\alpha = 0°$.

2.3.3.2 Electrorheological Composites

In this item, we shall consider a highly concentrated electrorheological liquid consisting of particles of goethite (wt. 45%), transformer oil (wt. 51%) and glycerol monooleate (wt. 4%). The viscoelastic properties of this ERC elaborated in the LRM of LHMTI strongly depend on the temperature. As seen from Figs. 2.13 and

Fig. 2.13 Storage modulus G'_{v} vs. electric field strength $\mathcal{E}$ for the ERC with 45 % of the mass concentration of disperse phase.

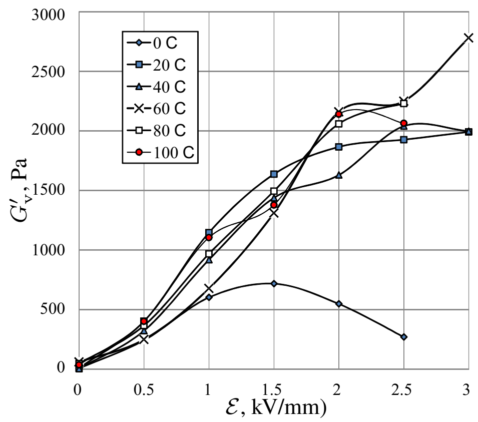

2.14, the storage and loss moduli, G'_{v} and G''_{v}, increase together with the electric field strength $\mathcal{E}$ at all the interval from 0 to 2 kw/mm for any temperature from 20 to 80° C. At the zeroth temperature, the electrorheological activity of the dispersed phase is very low. At temperature 100° C, the effect of electric field drops. And the highest electrorheological activity is observed at 60° C: the moduli G'_{v}, G''_{v} are monotonically increasing functions of the electric field strength and reach large values (2779 and 504 kPa, respectively) for $\mathcal{E} = 3$ kw/mm.

Fig. 2.14 Loss modulus G''_{v} vs. electric field strength $\mathcal{E}$ for the ERC with 45 % of the mass concentration of disperse phase.

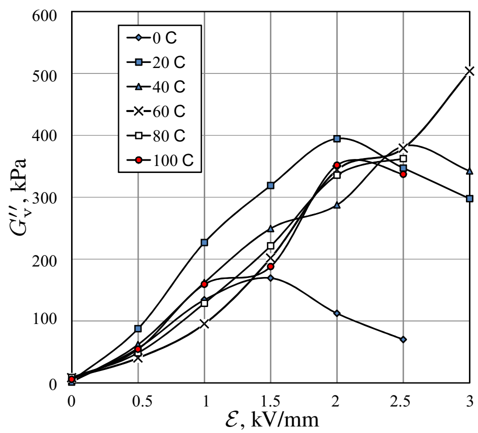

2.3.3.3 Magnetorheological Fluids

We consider also three samples of magnetorheological fluids, MRF-1, MRF-2 and MRF-3, with the same percentage of iron particles in an oil (wt. 80%), but differing in particle size (s. Table 2.7). The elastic and rheological properties of these smart liquids elaborated in the LRM of LHMTI are presented in Tables 2.8-2.10.

The analysis of the loss factor η_{V} for all MRFs shows that in the absence of a magnetic field the MRF-1 with more large iron particles behaves as a less viscous liquid. When the value of the field induction exceeds 200 mT, there is the tendency of decreasing the value of η_{V} and the predominance of the elastic properties of the system as a whole.

When comparing all the smart magnetorheological materials presented above, one can see that for MRFs the increase in the magnetic field does not give a very large increment in the storage and loss moduli, which is characteristic of MREs. At the same time, MRFs posses the largest loss factor at the entire range of variation of a magnetic field induction.

The elastic and viscous properties of VSMs considered in this section will be used below for simulation of damping vibrations of the MRE/ERC/MRF-based laminated beams, plates and shells. It will be shown also that besides damping capabilities similar VSMs posses capacity to control the total stiffness of thin-walled structures and thus increase their load-carrying capability.

In what follows, all smart materials given in this section, except for MRE-2, will be treated as isotropic ones.

Table 2.7 Disperse phase of MRFs.

Sample	Graded of main component	Particle diameter, μm
MRF-1	S-1000	13
MRF-2	S-3700	3
MRF-3	S-3500	2

Table 2.8 The storage and loss moduli G'_{V}, G''_{V} and loss factor η_{V} vs. the magnetic induction B for the MRF-1.

Magnetic induction B, mT	Storage modulus G'_{V}, kPa	Loss modulus G''_{V}, kPa	Loss factor η_{V}
0	3.14	2.3	0.744
50	56.5	36.9	0.653
100	174.9	76.8	0.439
150	354.7	139.4	0.393
200	443.0	169.2	0.382
250	659.6	186.0	0.282
300	725.3	129.1	0.178
350	728.7	97.6	0.134

Table 2.9 The storage and loss moduli $G'_{\rm v}$, $G''_{\rm v}$ and loss factor $\eta_{\rm v}$ vs. the magnetic induction B for the MRF-2.

Magnetic induction B, mT	Storage modulus $G'_{\rm v}$, kPa	Loss modulus $G''_{\rm v}$, kPa	Loss factor $\eta_{\rm v}$
0	17.1	30.9	1.808
50	32.6	34.8	1.068
100	59.2	42.2	0.713
150	106.7	47.7	0.447
200	177.9	78.6	0.442
250	255.6	68.5	0.268
300	339.2	76.3	0.225
350	436.1	90.7	0.208

Table 2.10 The storage and loss moduli $G'_{\rm v}$, $G''_{\rm v}$ and loss factor $\eta_{\rm v}$ vs. the magnetic induction B for the MRF-3.

Magnetic induction B, mT	Storage modulus $G'_{\rm v}$, kPa	Loss modulus $G''_{\rm v}$, kPa	Loss factor $\eta_{\rm v}$
0	34.0	29.6	0.870
50	43.0	35.7	0.830
100	91.9	63.9	0.695
150	102.4	48.8	0.477
200	166.5	77.9	0.468
250	262.3	72.4	0.276
300	352.6	68.8	0.195
350	454.6	84.6	0.186
400	677.9	122.0	0.180
450	696.3	122.5	0.176

2.3.4 Governing Equations for Smart Cylindrical Shells

The differential equations derived in Sect. 2.2 may be adapted for the case when some of layers are made of viscoelastic material (Mikhasev et al, 2011). Let the $k^{\rm th}$ lamina be fabricated from a VSM described above. When assuming the harmonic (sinusoidal) dynamic response of a shell, the viscoelastic properties of this layer may be represented by the complex form (2.163) for Young's and shear moduli.

As mentioned above, many of VSMs possessing isotropy in absence of external magnetic or electric field, show anisotropic properties at high level of applied electromagnetic signal. For a thick layer this property has an essential effect on the modes for which the amplitudes of the tangential and normal displacements of a shell have the same order. But the thinner the VSM-based layer is, the less anisotropy affects the dynamic behaviour of a laminated shell. We assume everywhere that a thickness of each layer composing a laminated shell is sufficiently small with respect to the characteristic size R of a structure. In what follows, considering dynamic problems we will analyze only small flexural vibrations taking into account shear deformations. Then a viscoelastic layer may be assumed to be transversally isotropic. In this case, the complex moduli E_k and G_k for the $k^{\rm th}$ viscoelastic layer are coupled by

Eq. (2.165). For many elastomeric materials, Poison's ratio ν_{v} is about $0,4$ (White and Choi, 2005). Aguib et al (2014) consider a MRE (see above propereties for MRE-2) as a material closed to incompressible and assume $\nu_{\mathrm{v}} \approx 0.45$. We also consider Poisson's ratio ν_k for the k^{th} viscoelastic layer as a real parameter in the range from 0.4 to 0.45.

Because the moduli E_k and G_k are the complex magnitudes for the VSM-based layers, all coefficients appeared in the governing equations becomes complex functions of the magnetic induction B or electric field strength $\mathcal{E}$. In particular, the reduced Poisson's ratio ν, Young's modulus E, shear parameter β, bending stiffness D, and dimensionless stiffness γ_k defined by Eqs. (2.14), (2.18), (2.84), (2.88) and (2.19), respectively, will be complex. If a magnetic or electric field is not stationary, then they are complex function of time. In addition, due to different exposure of the external magnetic/electric field on different parts of the VSM-based layer, above complex magnitudes may depend on the curvilinear coordinates α_1, α_2.

The accuracy of the governing equations derived in Sect. 2.1 was formally discussed in Subsect. 2.1.13. However, the estimation of an error of the equivalent single layer (ESL) model for a multi-layered shell remains by an unsolved problem. One can states that the stiff characteristics of all layers composing a thin-walled multi-layered structure have to be approximately of the same order. One of the principle parameters affecting the error of the ESL model is the dimensionless stiffness γ_k. To minimize the total error, the geometrical and physical parameters of layers should be chosen in such away that parameters $|\gamma_k|$ were approximately the same for all $k = 1, 2, \ldots, N$, where N is a number of layers. As seen from (2.19), this requirement is equivalent to the estimate

$$\frac{|E_k|}{|E_{k+1}|} \sim \frac{h_{k+1}}{h_k} \quad \text{for any} \quad k = 1, 2, \ldots, N. \tag{2.167}$$

This condition becomes essential for shells assembled form elastic and more soft viscoelastic layers. As examples, we estimate here the parameters $|\gamma_k|$ for two three-layered plates having the same thicknesses of layers and made of different MREs. Let the top and bottom of both sandwiches be made of the ABS-plastic SD-0170 with parameters $E_1 = E_3 = 1.5 \cdot 10^3$ MPa, $\nu_1 = \nu_3 = 0.4$, and cores are fabricated from the MRE-1 and MRE-5, respectively. The viscoelastic properties of these materials were specified above (s. Fig. 2.9 and Table 2.4). Figures 2.15 and 2.16 show the parameters $|\gamma_1| = |\gamma_3|$, $|\gamma_2|$ for both samples versus the magnetic induction B at the fixed thickness $h_1 = h_3 = 0.5$ mm of the elastic top and bottom layers and different thicknesses $h_2 = 5, 8, 11, 15$ mm of the viscoelastic cores. It is seen that at a small level of a magnetic field, the parameters $|\gamma_k|$ differ appreciably for both cases, and with the increase of induction B (from 0 to 200 mT for MRE-1 and from 200 to 800 mT for MRE-5), plots for $|\gamma_1| = |\gamma_3|$ and $|\gamma_2|$ approach to each other, from above and below, respectively. The rise of the core thickness (under the fixed thicknesses of outer and innermost layers) also effects the stiff characteristics γ_k: the larger h_2 is, the faster values of $|\gamma_{1,3}|$ and $|\gamma_2|$ approach each other with increasing magnetic field. When comparing two types of MRE, one can conclude: for the MRE-5 based sandwich, condition (2.167) is satisfied better, whereas for the

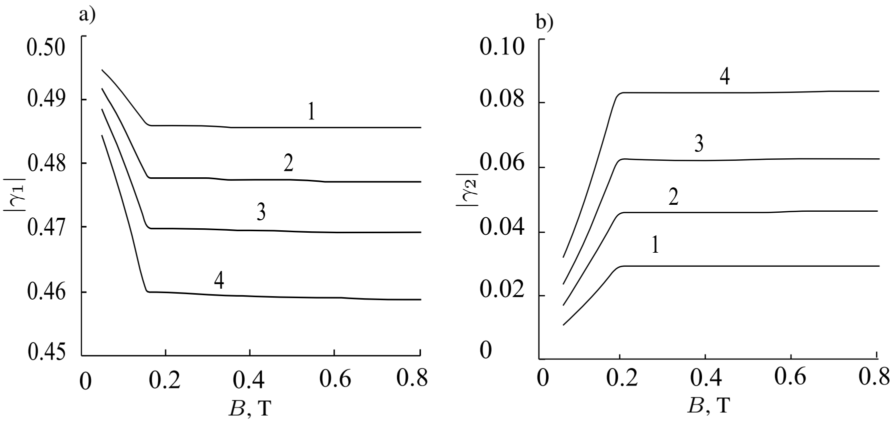

Fig. 2.15 Dimensionless stiffness parameters: a) $|\gamma_1| = |\gamma_3|$ and b) $|\gamma_2|$ vs. magnetic field induction B for MRE-1 at different thicknesses h_2 of the MRE-1 core: 1 - $h_2 = 5$ mm, 2 - $h_2 = 8$ mm, 3 - $h_2 = 11$ mm, 4 - $h_2 = 15$ mm.

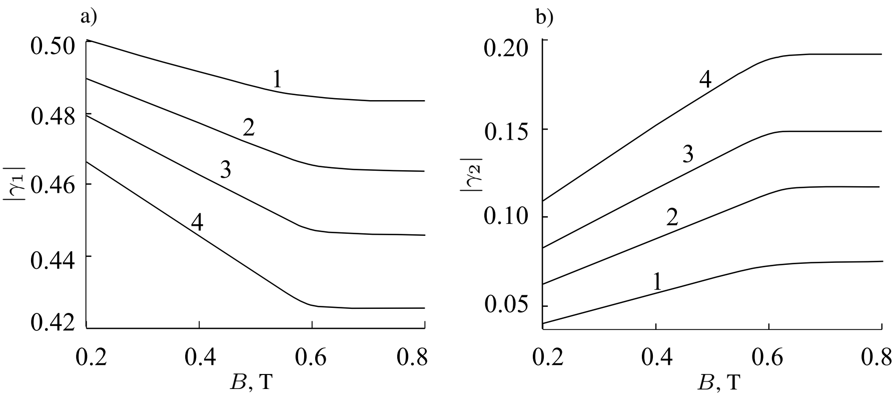

Fig. 2.16 Dimensionless stiffness parameters: a) $|\gamma_1| = |\gamma_3|$ and b) $|\gamma_2|$ vs. magnetic field induction B for MRE-5 at different thicknesses h_2 of the MRE-5 core:1 - $h_2 = 5$ mm, 2 - $h_2 = 8$ mm, 3 - $h_2 = 11$ mm, 4 - $h_2 = 15$ mm.

sample with the MRE-1 based core, this requirement can be reached by only further increment in the core thickness.

2.4 Finite Element Analysis

As mentioned above, the accurate estimate of an error of all equations derived in this chapter is still a subject for subsequent investigations. That is why it is a very important to have an alternative approach to compare solutions of problems found by different methods. The finite element method (FEM) is expected as the alternative and universal method permitting to evaluate the applicability of the governing equations and the ESL model in whole being developed in this book.

In the next chapters, to analyze buckling or vibrations of laminated cylindrical shell we will use the *SemiLoof* element family of the general purpose finite element package COSAR (Gabbert and Altenbach, 1990). The *SemiLoof* elements have been preferred due to their good overall accuracy in most shell applications and robustness compared with other possible finite shell elements. Originally, the *SemiLoof* element family was proposed by Irons (1976). The elements consists of 24 and 32 degrees of freedom (*dof*) for a curved six node triangular and an eight node quadrilateral element, respectively. These *dof* are the three displacements at each node, and additionally, the two tangential rotations at the two Gaussian integration points on each edge. The displacements and rotations are approximated by two families of shape functions, *Lagrange* polynomials are used for the displacements and *Legendre* polynomials are employed for the rotations. The element has $C^{(0)}$ continuity along the edges and a poitwise $C^{(1)}$continuity at the *Loof*-nodes (the two *Gaussian* integration points on the edges). The element fulfils the patch test.

In order to simulate different material layers the classical laminate theory (CLT) is used. For buckling analysis a second order theory is utilized (classical stability problem) to calculate the critical eigenvalues from the eigenvalue problem

$$(\mathbf{K}_{\mathrm{s}} - \lambda \mathbf{K}_{\sigma})\mathbf{u} = \mathbf{0} \tag{2.168}$$

with the stiffness matrix $\mathbf{K}_{\mathrm{s}}$, the geometric or initial stress matrix $\mathbf{K}_{\sigma}$ and the eigenvalue λ.

In stability problem (3.22), a single parameter load is considered where the critical stress state σ_{c} (first critical buckling point) is calculated from an initial stress state $\hat{\sigma}$ as

$$\sigma_{\mathrm{c}} = \lambda \hat{\sigma} \tag{2.169}$$

caused by the initial load state.

The initial stress state $\hat{\sigma}$ is calculated from a first linear solution of the cylindrical shell under the initial load state. In a second step the eigenvalue problem equation (3.22) is solved where the eigenvalue λ is the load parameter. The matrix $\mathbf{K}_{\sigma}$ is assembled from the following geometric element stiffness matrices (Zienkiewicz, 1977)

$$\mathbf{K}_{\sigma}^{(\mathrm{e})} = \int\limits_{V} \mathbf{G}_{u}^{\mathrm{T}} \hat{\sigma} \mathbf{G}_{u} \mathrm{d}V \tag{2.170}$$

where $\mathbf{G}_{u}$ contains the displacement gradient expressed by the shape function. The solution of the eigenvalue problem (2.168) results in the load factor λ, and the critical load level can be calculated by equation (2.169).

For a vibration analysis of elastic laminated shells the eigenvalue problem

$$(\mathbf{K}_{\mathrm{s}} - \omega^2 \mathbf{M}_{\sigma})\mathbf{u} = \mathbf{0} \tag{2.171}$$

has to be solved, where $\mathbf{M}$ is the mass matrix, and ω is the eigenfrequency.

References

Aguib S, Noura A, Zahloul H, Bossis G, Chevalier Y, Lançon P (2014) Dynamic behavior analysis of a magnetorheological elastomer sandwich plate. Int J Mech Sc 87:118–136

Alfutov NA (2000) Stability of Elastic Structures. Foundations of Engineering Mechanics, Springer, Berlin, Heidelberg

Bert CW (1947) Material damping: Introductory review of mathematic measures and experimental technique. J Sound Vibr 29(2):129–153

Bica I, Anitas EM, Bunoiu M, Vatzulik B, Juganaru I (2014) Hybrid magnetorheological elastomer: Influence of magnetic field and compression pressure on its electrical conductivity. J Indust Engng Chem 20(6):3994–3999

Bica I, Anitas EM, Averis LME, Bunoiu M (2015) Magnetodielectric effects in composite materials based on paraffin, carbonyl iron and graphene. J Indust Engng Chemist 21:1323–1327

Biot MA (1958) Linear thermodynamics and the mechanics of solids. In: Haythornthwaite RM (ed) Proc. of the Third U.S. National Congress on Applied Mechanics, ASME, New York, pp 1–18

Boczkowska A, Awietjan SF, Pietrzko S, Kurzydlowski KJ (2012) Mechanical properties of magnetorheological elastomers under shear deformation. Comp: Part B 43:636–640

Bolotin VV (1956) Dynamic Stability of Elastic Systems (in Russ.). Gostekhizdat, Moscow

Boltzmann L (1878) Zur Theorie der elastische Nachwirkung. Annalen der Physik lind Cbemie Suppl 241(11):430–432

Chen L, Gong XL, Jiang WQ, Yao JJ, Deng HX, Li WH (2007) Investigation on magnetorheological elastomers based on natural rubber. J Material Sc 42(14):5483–5489

Chen L, Gong XL, Li WH (2008) Effect of carbon black on the mechanical performances of magnetorheological elastomers. J Polymer Testing 27(3):340–345

Cosson P, Michon JC (1996) Identification by a non-integer order model of the mechanical behaviour of an elastomer. Chaos, Solutions and Fractals 7(11):1807–1824

Demchuk SA, Kuzmin VA (2002) Viscoelastic properties of magnetorheological elastomers in the regime of dynamic deformation. J Engng Phys Thermophys 75(2):396–400

DiTaranto RA (1965) Theory of vibratory bending for elastic and viscoelastic layered finite-length beams. Trans ASME J Appl Mech 32(4):881–886

Donnell LH (1976) Beams, Plates and Shells. McGraw-Hill Inc, New York

Douglas BE, Yang JCS (1978) Transverse compressional damping in the vibratory response of elastic-viscoelastic beams. AIAA J 16(9):925–930

Farshad M, Benine A (2004) Magnetoactive elastomer composites. Polymer Testing 23(3):347–353

Fung YC, Sechler EE (1974) Thin-Shell Structures: Theory, Experiments, and Design. Prentics-Hall, New Jersey

Gabbert U, Altenbach J (1990) COSAR - A reliable system for research and application (in Germ.). Technische Mechanik 11(3):125–137

Ginder GM, Schlotter WF, Nichhols ME (2001) Magnetorheological elastomers in tunable vibration absorbers. Proc SPIE 3985:103–110

Gol'denveizer AL (1961) Theory of Thin Elastic Shells. International Series of Monograph in Aeronautics and Astronautics, Pergamon Press, New York

Gol'denveizer AL, Lidsky VB, Tovstik PE (1979) Free Vibrations of Thin Elastic Shells (in Russ.). Nauka, Moscow

Grigolyuk EI, Kabanov VV (1978) Stability of Shells (in Russ.). Nauka, Moscow

Grigolyuk EI, Kulikov GM (1988) Multilayered Reinforced Shells. Calculation of Pneumatic Tires (in Russ.). Mashinostroenie, Moscow

Gross B (1947) On creep and relaxation. J Appl Phys 18(2):212–221

Hao T, Kawai A, Ikazaki F (1998) Mechanism of the electrorheological effect: evidence from the conductive, dielectric, and surface characteristics of water-fee electrorheological fluids. Langmuir 14(5):1256–1262

Hu YC, Huang SC (2000) The frequency response and damping effect of three-layer thin shell with viscoelastic core. Comp Struct 76(5):577–591

Irons BM (1976) The semiloof shell element. In: Ashwell DG, Gallagher R (eds) Finite Elements for Thin Shells and Curved Membranes, Wiley, New York, pp 197–222

Jin G, Yang C, Liu Z, Gao S, Zhang C (2015) A unified method for the vibration and damping analysis of constrained layer damping cylindrical shells with arbitrary boundary conditions. Comp Struct 130:124–142

Kallio M, Lindroos T, Aalto S, Karna T, Meinander T (2007) Dynamic compression testing of a tunable spring element consisting of a magnetorheological elastomer. Smart Mater Struct 16(2):506–514

Kervin Jr EM (1959) Damping of flexural waves by a constrained viscoelastic layer. The J Acoust Soc Am 31(7):952–962

Khatri KN (1996) Axisymmetric vibration of multilayered conical shells with core layers of viscoelastic material. Comp & Struct 58(2):389–406

Kimball AL, Lovell DE (1927) Internal friction in solids. Phys Rev Ser 2(30):948–959

Koeller RC (1984) Application of fractional calculus to the theory of viscoelasticity. Trans ASME J Appl Mech 51(2):299–307

Koiter WT (1966) On the nonlinear theory of thin elastic shells. Proc Koninkl Acad Westenschap B69:1–54

Korobko EV, Zhurauski MA, Novikova ZA, Kuzmin VA (2009) Rheological properties of magnetoelectrorheological fluids with complex disperse phase. J Phys: Conf Ser 149(1):012,065

Korobko EV, Mikhasev GI, Novikova ZA, Zurauski MA (2012) On damping vibrations of three-layered beam containing magnetorheological elastomer. Journal of Intelligent Material Systems and Structures 23(9):1019–1023

Kumar N, Singh SP (2010) Governing equations for vibrating constrained-layer damping sandwich plates and beams. Comp Struct 92(2):233–243

Kumar V, Lee DJ (2017) Iron particle and anisotropic effects on mechanical properties of magneto-sensitive elastomers. Journal of Magnetism and Magnetic Materials 441:105 – 112

Lavrent'ev MA, Ishlinsky AJ (1949) Dynamical modes of stability loss of elastic systems. Doklady Physics 64(6):776–782

Li WH, Zhou Y, Tian TF (2009) Sensing behavior of magnetorheological elastomers. J Mech Des 113(9):091,004–6

Li WH, Zhou Y, Tian TF (2010) Viscoelastic properties of mr elastomers under harmonic loading. Rheol Acta 49(7):733–740

Lu YP, Killian JW, Everstine GC (1979) Vibrations of three layered damped sandwich plate composites. J Sound Vibr 64(1):63–71

Matter M, Gmür T, Cugnoni J, Schorderet A (2011) Identification of the elastic and damping properties in sandwich structures with a low core-to-skin stiffness ratio. Comp Struct 93(2):331–341

Mead DJ, Ae DC (1960) The effect of a damping compound on jet-efflux excited vibrations: an article in two parts presenting theory and results of experimental investigation. Part I. The structural damping due to the compound. Aircraft Engineering and Aerospace Technology 32(3):64–72

Mead DJ, Markus S (1969) The forced vibration of a three-layer, damped sandwich beam with arbitrary boundary conditions. J Sound Vibr 10(2):163–175

Mead DJ, Markus S (1970) Loss factors and resonant frequencies of encastrè damped sandwich beams. J Sound Vibr 12(1):99–112

Mikhasev G, Botogova M, Korobko E (2011) Theory of thin adaptive laminated shells based on magnetorheological materials and its application in problems on vibration suppression. In: Altenbach H, Eremeyev V (eds) Shell-like Structures, Springer, Heidelberg, Advanced Structured Materials, vol 15, pp 727–750

Mikhasev GI (2016) Edge effect equations in the theory of thin laminated transversally-isotropic cylindrical shells with low shear stiffness (in Russ.). Vestnik BGU, Serie 1: Fiz Mat Inform 8(3):148–153
Mikhasev GI, Botogova GI (2017) Effect of edge shears and diaphragms on buckling of thin laminated medium-length cylindrical shells with low effective shear modulus under external pressure. Acta Mechanica 228(6):2119–2140
Morozov NF, Tovstik PE (2010) On modes of buckling for a plate on an elastic foundation. Mechanics of Solids 45(4):519–528
Mushtari K, Galimov K (1961) Nonlinear Theory of Thin Elastic Shells. NSF-NASA, Washington
Novozhilov V (1970) Theory of Thin Shells. Wolters-Noordhoff, Groningen
Oberst H, Frankenfeld K (1952) Über die Dämpfung der Biegeschwingungen dünner Bleche durch fest haftende Beläge. Acta Acustic united with Acustica 14(2, Suppl. 4):181–194
Pan HH (1969) Axisymmetrical vibrations of a circular sandwich shell with a viscoelastic core layer. J Sound Vibr 9(2):338–348
Parke S (1966) Logarithmic decrements at high damping. Brit J Appl Phys 17(2):271–273
Qatu MS, Sullivan RW, Wang W (2010) Recent research advances on the dynamic analysis of composite shells: 2000-2009. Comp Struct 93(1):14–31
Raamesh TC, Ganesan N (1994) Orthotropic cylindrical shells with a viscoelastic core: A vibration and damping analysis. J Sound Vibr 175(4):535–555
Rao MD, He S (1992) Analysis of natural frequencies and modal loss factors of simply supported beams with double-strap joints. J Acoust Soc Am 92(1):268–276
Ross D, Ungar EE, Kerwin EM (1959) Damping of flexural vibrations by means of viscoelastic laminae. In: Ruzicka JE (ed) Structural Damping, ASME, pp 49–87
Saravanan C, Ganesan N, Ramamurti V (2000) Vibration and damping analysis of multilayered fluid filled cylindrical shells with constrained viscoelastic damping using modal strain energy method. Comp Struct 75(4):395–417
Scanlan RH, Rosenbaum R (1951) Introduction to the Study of Aircraft Vibration and Flutter. Macmillan, New York
Schwaar M, Gmür T, Frieden J (2011) Modal numerical-experimental identification method for characterising the elastic and damping properties in sandwich structures with a relatively stiff core. Comp Struct 94(7):2227–2236
Soroka WW (1949) Note on the relations between viscous and structural damping coefficients. J Aeronautical Sc 16(7):409–410
Srubschik L (1988) Dynamical buckling of elastic shells under action of pulse loading. J Appl Math Mech 51(1)
Srubschik LS (1985) Energetic test of dynamical buckling of spherical shells. Soviet Phys Dokl 280(1)
Stepanov GV, Abramchuk SS, Grishin DA, Nikitin L, Kramarenko EY, Khokhlov AR (2007) Effect of a homogeneous magnetic field on the viscoelastic behavior of magnetic elastomers. Polymer 48(2):488–495
Sun TL, Gong XL, Jiang WQ, Li JF, Xu ZB, Li WH (2008) Study on the damping properties of magnetorheological elastomers based on cis-polybutadiene rubber. Polymer Testing 27(4):520–526
Tovstik PE (2005) Local buckling of plates and shallow shells on an elastic foundation. Mechanics of Solids 40(1):120–121
Tovstik PE, Smirnov AL (2001) Asymptotic Methods in the Buckling Theory of Elastic Shells. World Scientific, Singapore
Ungar EE, Kerwin Jr EM (1962) Loss factors of viscoelastic systems in terms of energy concepts. J Acoust Soc Am 34(7):954–957
Venkateswara RP, Maniprakash S, Srinivasan SM, Srinivasa AR (2010) Functional behavior of isotropic magnetorheological gels. Smart Mater Struct 19(8):085,019
Vol'mir AS (1972) Nonlinear Dynamics of Plates and Shells (in Russ.). Nauka, Moscow
Vol'mir AS (1976) Shells in a Liquid and Gas Flow. Problems of Aeroelasticity (in Russ.). Nauka, Moscow

Volterra E (1950) Vibrations of elastic systems having hereditary characteristics. Trans ASME J Appl Mech 17:363–371

Wang HJ, Chen LW (2004) Finite element dynamic analysis of orthotropic cylindrical shells with a constrained damping layer. Finite Elements in Analysis and Design 40(7):737–755

Wang YL, Hu Y, Deng HX, Gong XL, Zhang PQ, Jiang WQ, Chen Z (2006) Magnetorheological elastomers based on isobutylene-isoprene rubber. Polymer Engng & Sc 46(3):264–268

White J, Choi D (2005) Polyolefin. Processing, Structure, Development, and Properties. Carl Hanser, Munich

Wiess KD, Carlson JD, Nixon DA (1994) Viscoelastic properties of magneto- and electro-rheological fluids. J Intell Mater Syst Struct 5(6):772–775

Wlassow WS (1958) Allgemeine Schalentheorie und ihre Anwendung in der Technik. Akademie-Verlag, Berlin

Yan MJ, Dowell EH (1972) Governing equations for vibrating constrained-layer damping sandwich plates and beams. Trans ASME J Appl Mech 39(4):1041–1046

Yang IH, Yoon JH, Jeong JE, Jeong UC, Kim JS, Chung KH, Oh JE (2013) Magnetic-field-dependent shear modulus of a magnetorheological elastomer based on natural rubber. J Korean Phys Soc 62(2):220–228

Yu SC, Huang SC (2001) Vibration of a three-layered viscoelastic sandwich circular plate. Int J Mech Sc 43(10):2215–2236

Zajac P, Kaleta J, Lewandowski D, Gasperowicz A (2010) Isotropic magnetorheological elastomers with thermoplastic matrices: structure, damping properties and testing. Smart Mater Struct 19(4):045,014

Zhou H, Rao MD (1996) Damping of composite tubes with embedded viscoelastic layers. ASME J Vib Acoust 118(3):384–389

Zhou XQ, Yu DY, Shao X, Wang S, Zhang SQ (2015) Simplified-super-element-method for analyzing free flexural vibration characteristics of periodically stiffened-thin-plate filled with viscoelastic damping material. Thin-Walled Structures 94:234–252

Zhurauski MA, Dragašius E, Korobko EV, Novikova ZA (2008) Mechanical properties of smart fluids under combined electric and magnetic fields. Mechanika 6(74):21–24

Ziegler H (1968) Principles of Structural Statbility. Blaisdell Publ. Comp, Waltham, Massachusetts

Zienkiewicz OC (1977) The Finite Element Method. McGraw Hill Book Company Limited, New York